frontiers in Earth Science

ORIGINAL RESEARCH
published: 03 January 2022
doi: 10.3389/feart.2021.751216

Selected Crater and Small Caldera Lakes in Alaska: Characteristics and Hazards

*Christopher F. Waythomas**

US Geological Survey, Alaska Volcano Observatory, Anchorage, AK, United States

This study addresses the characteristics, potential hazards, and both eruptive and non-eruptive role of water at selected volcanic crater lakes in Alaska. Crater lakes are an important feature of some stratovolcanoes in Alaska. Of the volcanoes in the state with known Holocene eruptive activity, about one third have summit crater lakes. Also included are two volcanoes with small caldera lakes (Katmai, Kaguyak). The lakes play an important but not well studied role in influencing eruptive behavior and pose some significant hydrologic hazards. Floods from crater lakes in Alaska are evaluated by estimating maximum potential crater lake water volumes and peak outflow discharge with a dam-break model. Some recent eruptions and hydrologic events that involved crater lakes also are reviewed. The large volumes of water potentially hosted by crater lakes in Alaska indicate that significant flowage hazards resulting from catastrophic breaching of crater rims are possible. Estimates of maximum peak flood discharge associated with breaching of lake-filled craters derived from dam-break modeling indicate that flood magnitudes could be as large as 10^3–10^6 m^3/s if summit crater lakes drain rapidly when at maximum volume. Many of the Alaska crater lakes discussed are situated in hydrothermally altered craters characterized by complex assemblages of stratified unconsolidated volcaniclastic deposits, in a region known for large magnitude (>M7) earthquakes. Although there are only a few historical examples of eruptions involving crater lakes in Alaska, these provide noteworthy examples of the role of external water in cooling pyroclastic deposits, acidic crater-lake drainage, and water-related hazards such as lahars and base surge.

Keywords: Alaska, crater lakes, hazards, floods, eruptions

OPEN ACCESS

Edited by:
Dmitri Rouwet,
Istituto Nazionale di Geofisica e Vulcanologia, Italy

Reviewed by:
Vern Manville,
University of Leeds, United Kingdom
Valerio Acocella,
Roma Tre University, Italy

***Correspondence:**
Christopher F. Waythomas
cwaythomas@usgs.gov

Specialty section:
This article was submitted to Volcanology, a section of the journal Frontiers in Earth Science

Received: *31 July 2021*
Accepted: *11 October 2021*
Published: *03 January 2022*

Citation:
Waythomas CF (2022) Selected Crater and Small Caldera Lakes in Alaska: Characteristics and Hazards. Front. Earth Sci. 9:751216. doi: 10.3389/feart.2021.751216

1 INTRODUCTION

Volcanic crater lakes are distinguishing features of many active stratovolcanoes in Alaska and elsewhere (Christenson et al., 2015). Crater lakes commonly form after crater-forming eruptions where local volcanic and hydrologic conditions permit the development of confined lakes within the crater itself. Eruptions through crater lakes pose a special type of hazard because of the potential for explosivity associated with magma-water interaction and the possibility for voluminous water-rich mass flows that can develop if lake water is explosively expelled from its host crater or produced by catastrophic breaching of the crater wall (Mastin and Witter, 2000; Manville et al., 2007). The hazards associated with volcanic crater lakes beyond Alaska have received some study especially in locations where people and infrastructure are at risk (Mastin and Witter, 2000; Manville, 2010; Manville, 2015, and references therein). In New Zealand, partial failure of the rim of Crater Lake at Mount Ruapehu in 1953 caused a significant flood and lahar that resulted in 151 fatalities (Manville et al., 2007)

FIGURE 1 | Location of crater and small caldera lakes in Alaska discussed in this study. The Alaska Peninsula is abbreviated AK Pen.

highlighting the importance of catastrophic crater lake drainage. These works and others (Neall, 1996; Strehlow et al., 2017; Rouwet, 2021) have noted the hazard implications of large volumes of water within the craters of active volcanoes and this is in part the motivation to evaluate hydrologic hazards at crater lakes in Alaska.

In Alaska, volcanic craters that contain lakes are present at several locations throughout the Aleutian Arc (**Figure 1**). However, the hydrologic hazards and consequences of eruptions involving these lakes have received little study. The volume of water present in existing crater lakes in Alaska (**Table 1**) indicates that there could be significant hydrologic consequences associated with eruptive activity through water, or failure of crater rims. To address potential hazards and lake water eruption interactions, existing information about a representative sampling of crater and small caldera lakes in Alaska is synthesized and the potential hydrologic hazards associated with failure of crater walls leading to large dam-break type floods is evaluated. Not all crater and caldera lakes in the Aleutian arc are included here. The sampling of study locations provides examples of the main types of crater or potential crater lake settings found in Alaska. Maar craters are also not evaluated because they are uncommon in Alaska, although a maar crater lake drainage event did occur in Aniakchak caldera (McGimsey et al., 2014). Information about some plausible hydrologic hazards associated with drainage of lakes at Okmok and Aniakchak can be found in Larsen et al. (2015) and Neal et al. (2001). Several recent Alaska examples of eruptions and hydrologic events that involved crater lakes also are reviewed to illustrate the role of lake water in influencing eruptive processes and hazardous hydrologic phenomena.

To date, there has been no systematic examination of crater lakes in the Aleutian Arc and thus the potential consequences of water bodies situated at the summit of active high-relief stratovolcanoes are not specifically known. The goal of this work is to establish some of the physical parameters involved with catastrophic release of water from crater lakes and to present examples of recent unrest where crater lakes had or were suspected of playing an important role during unrest. The first part of the study will address breaching of crater rims and associated water floods using a dam-break modeling approach. The second part of the study will focus on lake water involvement in the eruption process and associated hazards. Recent unrest at Kasatochi, Korovin, Makushin, and the north crater of Cerberus volcano, in Alaska (**Figure 1**) have raised numerous questions about the role and fate of external water in augmenting potential hazards during explosive eruptive activity and provide further motivation for this study. Although many of the drainages downstream from crater lakes described here are uninhabited with little infrastructure, these areas are visited seasonally and some contain significant biological resources (fish, wildlife, and habitat) that could be adversely affected by floods originating at crater lakes (Schaefer et al., 2008).

The volcanic craters discussed here are <1 km in diameter which roughly differentiates them from calderas which are larger (Francis, 1976). In Alaska, crater lakes are somewhat uncommon among the historically active volcanoes in the Aleutian Arc and of the volcanoes active during the Holocene, roughly one-third have summit crater lakes (**Table 1**), including two which are small caldera lakes (Katmai, Kaguyak). Kaguyak volcano has a summit caldera that is slightly larger than 1 km in diameter but is included here because it contains a large lake whose surface is close to a pronounced low point along the caldera rim (**Figure 2**). The volcano also has a documented history of explosive dome-forming eruptions of Holocene age (Fierstein and Hildreth, 2008); should similar eruptions occur in the future, they likely would be capable of displacing lake water that could overtop the caldera rim.

Previous studies of Holocene calderas in the Aleutian Arc have identified evidence for large caldera lake floods associated with catastrophic breaching of caldera rims at Aniakchak, Okmok and Fisher calderas (Waythomas et al., 1996; Wolfe, 2001; Stelling et al., 2005). These examples and other large calderas in Alaska will not be discussed further here as the focus of this study is on crater lakes and small caldera lakes that

TABLE 1 | Characteristics of volcanic crater lakes in Alaska. Volume estimates made from IfSAR digital elevation data; * indicates volume estimate based on crater depth multiplied by crater area at the spillover elevation.[#] Indicates volume estimate based on formula for a truncated cone, $V = {}^{1}/_{3}\,\pi d\,[(r^2 + r)(R + R^2)]$ where V is volume, r is bottom radius, R is top radius at the spillover elevation and d is depth. [@] Indicates volume estimate derived from DEM raster volume calculation in Qgis. These estimates do not include the volume of modern lakes. Maximum potential crater lake volume in bold indicates value used in peak discharge calculation.

Volcano and timing of last known eruptive activity	Coordinates	Crater/ caldera area (m^2)	Maximum Crater/ caldera depth (m)	Modern lake area (m^2)	Maximum potential crater lake volume* (m^3)	Maximum potential crater lake volume[#] (m^3)	Maximum potential crater lake volume[@] (m^3)	Comments
Mount Spurr summit 5–6 ka	−152.251° W, 62.300° N	9×10^4	140	1.1×10^4	9.7×10^6	**8.6×10^6**	5.5×10^6	Crater lake is an ephemeral feature; present 2004–2006. Crater depth estimated from IfSar DEM.
Crater Peak 1992	−152.239° W, 61.265° N	3.6×10^5	40	5×10^4	1.4×10^7	1.3×10^7	**1.8×10^6**	Crater lake is an ephemeral feature; present 1978–1992. Crater depth estimated from IfSar DEM and is the minimum depth for lake spillover at the low point on the crater rim
Douglas Holocene?	−153.535° W,58.859° N	1.3×10^5	10	6.1×10^4	9.8×10^5	**1×10^6**	1.6×10^5	Area of crater at low point on crater rim = 97,672 m^2. Lake area is the average of four lake areas measured from satellite images obtained in 2012, 2014, 2019, and 2020
Kaguyak Holocene	−154.0245° W,58.6113° N	6.1×10^6	150	3.6×10^6	9×10^8	**8.3×10^8**	1.3×10^8	The modern lake has a volume of about 5×10^8 m^3
Katmai 1912	−155.2544° W 58.1946° N	9.4×10^6	470	5.4×10^6	3.5×10^9	**1.5×10^9**	2.1×10^8	The modern lake has a volume of at least 1×10^9 m^3
Mageik Holocene	−155.2544° W,58.1946° N	8.5×10^4	35	8.6×10^3	9×10^5	2.2×10^6	**3.1×10^5**	Area of crater at low point on crater rim = 25,710 m^2
Martin Holocene	−155.3566° W 58.1692° N	1.2×10^5	50	9.7×10^3	3.1×10^6	5.1×10^6	**1×10^6**	Area of crater at low point on crater rim = 62,019 m^2
Chiginagak Holocene	−156.9915° W,57.13348° N	2.1×10^5	40	9.4×10^4	2.9×10^6	**3.8×10^6**	1.3×10^6	Crater and lake area from 2009 satellite image.Area of crater at low point on crater rim = 73,400 m^2
Dana Holocene?	−161.2155° W 55.64205° N	2.7×10^6	40	5.8×10^5	2.3×10^7	**2.6×10^7**	3.6×10^5	The depth of the modern lake was estimated in the field
Hague Holocene	−161.9778° W 55.373074° N	1.6×10^5	90	1.3×10^4	1×10^7	1.3×10^7	**4.6×10^6**	Modern crater lake is ephemeral
Makushin 1995	−166.9320° W 53.88707° N	3.5×10^5	100	2.4×10^4	3.5×10^7	**1.9×10^6**	4.2×10^5	Dimensions from August 1, 2020, satellite image. Volume of modern lake unknown
Tana Holocene	−169.758° W 52.839° N	7.7×10^5	10	2.1×10^5	2.4×10^6	**3.4×10^6**	5.4×10^5	The volume of the modern lake is unknown
Herbert Holocene	−170.113° W 52.741° N	3.5×10^6	220	5.7×10^5	4.2×10^8	**3.5×10^8**	1.8×10^8	The volume of the modern lake is unknown
Korovin 1998	−174.1548° W 52.37934° N	3.7×10^5	140	1.6×10^4	3.6×10^7	9.4×10^6	**2.3×10^7**	Modern crater lake is ephemeral
Kasatochi 2008	−175.5113° W 52.1693° N	1.5×10^6	180	8.4×10^5	2.2×10^8	**2×10^8**	4.7×10^7	Dimensions based on November 22, 2020, satellite image
North crater, Cerberus 2021	−179.5856° W 51.935,588° N	1.5×10^7	120	$6–8 \times 10^3$	1.3×10^7	**7.4×10^6**	6.3×10^6	Modern crater lake is ephemeral

have no known catastrophic drainage events except for Chiginagak volcano which experiences repeated episodes of crater lake drainage (Schaefer et al., 2008).

2 METHODS

Crater and small caldera lakes in Alaska were evaluated using several approaches including consultation of photographic records, GIS analysis of digital elevation data, geologic maps, and previously published reports and articles. The methods and approaches used in this study are described briefly below and more fully in *Crater Stability and Susceptibility to Failure* and *Crater Rim Overtopping, Breach Formation, and Peak Flood Discharge*.

2.1 Historical Photographs of Crater Lakes in Alaska

The Alaska Volcano Observatory (AVO) has an extensive collection of photographs and satellite images of volcanoes throughout Alaska contributed by AVO scientists and other observers. This database (Cameron and Snedigar, 2016) was consulted for representative photographs of the crater and caldera lakes described in this paper. Most of the photographs are relatively recent images of the lakes and thus show the near

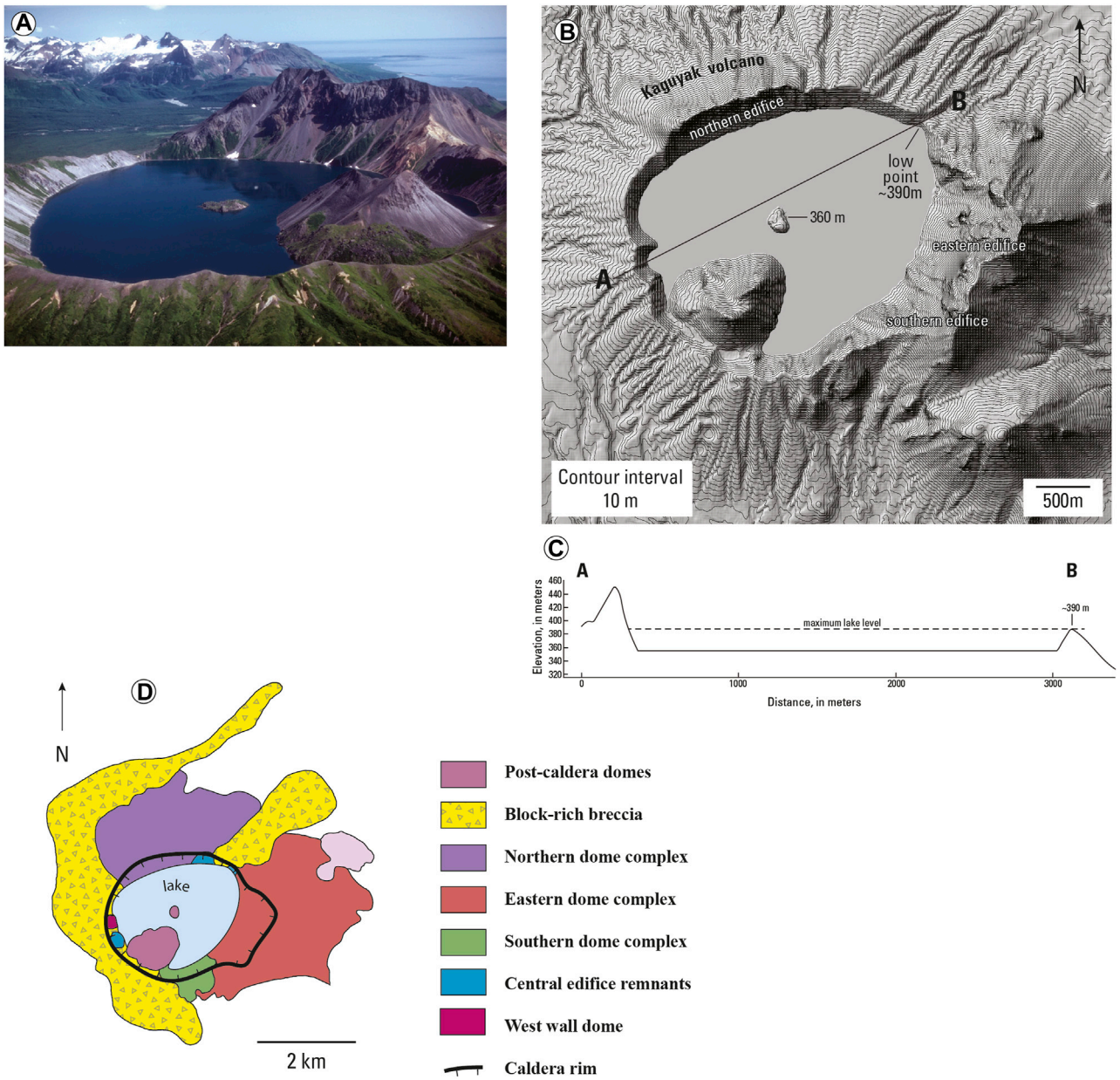

FIGURE 2 | Photograph, ifSAR derived topographic map, cross section, and generalized geologic map of Kaguyak caldera. **(A)**. Photograph of lake-filled caldera, August 1982. Photo by C.J. Nye, AVO. **(B)**. IfSAR derived topographic map of lake-filled caldera of Kaguyak volcano. **(C)**. Topographic profile from southwest to northeast across Kaguyak caldera. **(D)**. Generalized geologic map of Kaguyak volcano. Modified from Fierstein and Hildreth, 2008.

present configurations of the water bodies. Most of these photographs are shown in the **Supplementary Figures** that accompany this paper.

2.2 GIS Analysis and Volume Estimates of Crater Lakes

Spatial information about Alaska crater lakes is presented in the form of topographic maps and cross sections generated from 5 m-resolution ifSAR elevation data acquired 2012–2019 (Carswell, 2013). Digital elevation data for each crater lake was processed in Qgis where hillshade renderings and contour maps were constructed. The digital elevation data was used to identify the lowest point along the crater rim where spillover of lake water would likely occur, if the crater were filled to capacity. Topographic cross sections also were generated in Qgis through each crater rim low point; the cross sections provide a two-dimensional representation of each crater and are shown in the **Supplementary Figures** that accompany this paper. The maximum crater lake area was taken as the elevation contour

corresponding to the lowest point on the crater rim. The maximum potential lake depth was approximated as the elevation difference between the crater rim low point and the crater floor elevation including the lake depth if known or estimated. The maximum crater lake area multiplied by the depth gives a maximum theoretical lake volume estimate (**Table 1**) which is considered an upper bound on lake volume as this estimate does not explicitly account for crater geometry. A second volume estimate was made by assuming a truncated cone for crater shape and using the formula, $V = \frac{1}{3}\pi d[(r^2 + r)(R + R^2)]$ to calculate maximum water volume (V), where r is bottom radius, R is top radius at the spillover elevation, and d is depth. In many instances the volume estimates are about the same (**Table 1**) but in a few cases (Douglas, Makushin) the values differ by more than a factor of 10. Photographs of these two crater lakes indicate that the crater shapes are better approximated by a truncated cone so the volume estimates resulting from application of the truncated cone formula are used for these two volcanoes in subsequent calculations described below. A third maximum potential lake volume estimate was made using the ifSAR digital elevation data and the raster surface volume algorithm in Qgis. This method does not include the present lake volume, but where known gives volume estimates roughly comparable to the estimates made by the other two methods (**Table 1**). In most cases, application of the formula for a truncated cone, where the lake bottom elevation is known or reasonably approximated, gives the plausible estimates for maximum potential lake volume because qualitatively, many of the craters look like truncated cones. In cases where modern lakes are absent or small in volume, the Qgis raster volume estimates of maximum potential lake volume were used for subsequent calculations of maximum peak discharge because these estimates are based on actual ifSAR derived topography. The values used for peak discharge estimates are shown in bold in **Table 1**.

2.3 Previous Studies of Crater Geology

Published geologic information was consulted to make first-order evaluations of crater rim conditions to provide insight into crater wall geology, stability and susceptibility to erosion or failure. At many of the locations discussed, geologic information is limited or nonexistent. The specific reports and articles consulted are given as references throughout *Crater Lakes in Alaska*.

2.4 Assessment of Crater Rim Stability and Crater Lake Hydrology

Volcanic crater rim stability and susceptibility to failure are discussed in *Crater Stability and Susceptibility to Failure* of this paper. To date, there have been no rigorous evaluations of the strength of lake-filled craters using any of the standard approaches for determining rock-mass strength and slope stability (Watters et al., 2000). A first-order attempt to evaluate the seismic effects on crater wall stability is presented in *Seismic Effects on Volcanic Crater Lakes*. To date there have been no systematic studies of Alaska crater lake hydrology although some general conclusions about the hydrologic characteristics of the lakes are possible. These are described further in *Volcanic Crater Lake Hydrology*.

2.5 Dam-Break Modeling of Floods From Lake-Filled Volcanic Craters

The approach used to estimate maximum peak discharge associated with floods from lake-filled craters in Alaska is described in *Crater Rim Overtopping, Breach Formation, and Peak Flood Discharge*. This was done to benefit from the context established by the review of lake-filled volcanic craters in Alaska presented in *Crater Lakes in Alaska* and the analysis of crater rim stability and hydrology presented in *Crater Stability and Susceptibility to Failure*. The basic approach to dam-break analysis is described in Waythomas et al. (1996) but modified here for application to crater lakes.

3 SELECTED CRATER LAKES IN ALASKA

3.1 Mount Spurr Volcano

Mount Spurr volcano is in the Cook Inlet region of south-central Alaska (**Figure 1**). The volcano consists of a stratified assemblage of andesite lava flows and lahar, pyroclastic-flow, and debris-avalanche deposits of late Quaternary age (Nye and Turner, 1990). These rock units are truncated by a horseshoe-shaped avalanche caldera of Holocene age that is open to the southeast (**Supplementary Figure S1**). The summit cone of Mount Spurr is heavily glaciated and rock outcrops on the upper flanks of the volcano are largely obscured by snow and ice. The volume of ice and perennial snow on Mount Spurr when measured in 1981 was 67 ± 17 km^3 (March et al., 1997). A period of elevated heat flow at the summit in 2004–2006 resulted in partial exhumation of a crater on the summit edifice and formation of a small lake within the crater with an interior volume (**Supplementary Figure S1**; Coombs et al., 2006). By the end of this event, a crater about 9.7×10^6 m^3 was visible at the summit of the volcano. A small lake developed on the floor of the crater (first observed in 2004), covering an area of about 11,540 m^2 by 2006 (**Supplementary Figure S1**). The maximum volume of a hypothetical lake in the summit crater is $5.5–9.7 \times 10^6$ m^3 (**Table 1**). The thermal excursion of 2004–2006 is the only known period associated with the exhumation and formation of a crater lake at the Mount Spurr summit. Previous thermal events did occur that partially exposed the summit crater (Coombs et al., 2006) but no lakes were reported.

Crater Peak is a basaltic–andesite satellite cone on the south flank of Mount Spurr volcano (**Supplementary Figure S2**). Crater Peak has been the active vent of Mount Spurr volcano for about the past 5–6 ka (Riehle 1985) and was the site of the two documented historical eruptions in 1953 and 1992 (Keith, 1995). The first known historical eruption occurred on July 9, 1953 (Juhle and Coulter, 1955; Miller et al., 1998). It is unknown if a lake occupied the floor of Crater Peak prior to the 1953 eruption, but for several decades prior to the eruption, plumes of whitish steam commonly were observed

rising from the summit of Crater Peak and pilots reported an increase in the vigor of steaming in late spring 1953 (Juhle and Coulter, 1955). The 1953 eruption was a single explosive burst lasting about 1 hour, and it generated an ash cloud that rose more than 10 km above sea level (Juhle and Coulter, 1955).

Aerial photographs taken in 1952, 1954, and 1957 show no lake on the floor of Crater Peak (**Supplementary Figure S2**). A 1970 visit to Crater Peak indicated a hot lake was present in the crater (Keith et al., 1995). A Landsat satellite image acquired on July 27, 1974, also shows no lake on the crater floor. An aerial photograph taken on August 8, 1978, shows a lake present on the crater floor (**Supplementary Figure S2d**) and opportunistic photographs in the AVO photo database show a lake present from 1982 until the first Crater Peak eruption in 1992 on June 27. Intermittent observations of Crater Peak from 1992 to the present have indicated that a lake has not reformed after the 1992 eruption.

The low point on the crater rim is about 1940 m above sea level and the depth from the low point to the crater floor is about 40 m. The area of the crater is about 360,450 m^2 and the maximum volume of a crater-filling lake is about 1.8–14 × 10^6 m^3 (**Table 1**). Observations and photographic evidence indicate that at no time was the lake ever much more than a shallow feature on the floor of Crater Peak covering an area of about 50,000 m^2.

3.2 Mount Douglas

Mount Douglas is located on the west side of the marine entrance to Cook Inlet (**Figure 1**). Douglas is an ice- and snow-covered stratovolcano (summit altitude 2,140 m) with a summit crater that contains a small lake (**Supplementary Figure S3**). Little is known about the geologic history of Douglas volcano, and it is uncertain when the last eruption of the volcano occurred and when the summit crater developed. Measurements made in 1991 indicated that the lake had a temperature of 25°C and a pH of ~1 (Motyka et al., 1993). The summit crater has an area of about 134,000 m^2 and the crater lake covers an area of about 61,470 m^2 (average of four measurements made from satellite images, **Table 1**). The low point on the crater rim is about 10 m above lake level, and the maximum crater volume at this level is about 9.8–10 × 10^5 m^3 (**Table 1**).

3.3 Mount Chiginagak

Mount Chiginagak is an ice and snow-clad stratovolcano on the Alaska Peninsula near Mother Goose Lake (**Figure 1**). The volcano is about 8 km in diameter and its summit has an elevation of 2,135 m above sea level. The summit crater contains a lake (**Supplementary Figure S4**) that episodically drains through a glaciated breach on the crater rim (Schaefer et al., 2008). The volcano has had no known historical eruptive activity, although fumaroles on the upper flanks of the edifice are occasionally quite vigorous. The volcano developed during the late Quaternary and lava flows, lahar, pyroclastic, tephra and debris-avalanche deposits of Holocene and Pleistocene age characterize the edifice (Schaefer et al., 2017). Rocks in the summit area are hydrothermally altered although the type and extent are not known (**Supplementary Figure S4**; Schaefer et al., 2017).

The summit crater of Chiginagak volcano has an area of about 215,610 m^2 although a pronounced glacial notch in the rim (**Supplementary Figure S4**) precludes the entire crater becoming filled with water. The crater lake is an ephemeral feature that periodically develops when the heat flux through the upper edifice increases to melt snow and ice in the crater. As the lake level rises, the water encounters a glacier-occupied saddle (**Supplementary Figure S4**) that is the low point on the crater rim. At this elevation the maximum area a crater lake could attain is about 73,400 m^2 and the hypothetical lake volume is 1.3–3.8 × 10^6 m^3 (**Table 1**). Erosion of the ice dam allows, acidic lake water to flow from the crater and enter the Indecision Creek drainage on the west-northwest flank of the volcano (Schaefer et al., 2008). Acidic water floods are temporarily destructive to the riparian ecosystem of the Indecision Creek drainage including Mother Goose Lake (Schaefer et al., 2008).

3.4 Kaguyak Volcano

Kaguyak volcano and its defining caldera lake is a silicic volcanic center consisting of numerous nested lava domes and flows. The volcano is in Katmai National Park on the northeastern Alaska Peninsula (**Figure 1**). Kaguyak experienced a caldera-forming eruption about 5.8 ka (Fierstein, and Hildreth, 2008) and a lake formed in the small 2.5 × 3 km diameter caldera after the eruption. The lake is estimated to be about 150 m deep, has a surface area of 3.6 × 10^6 m^2 and an approximate volume of 5 × 10^8 m^3 (Fierstein and Hildreth, 2008). The caldera rim has a distinct low point where the lake spillover should occur if the water level increased by about 30 m (**Figure 2**). The maximum water volume the caldera could hold is 1.3–9 x 10^8 m^3 (**Table 1**). Information about modern lake level fluctuations is not known.

Kaguyak has had no known historical activity and the exposed walls of the caldera do not appear significantly altered. At least three nested dome complexes were identified by Fierstein and Hildreth (2008) that make up the bulk of the volcano (**Figure 2**). There are no outward signs of caldera rim instability although areas of edifice overlap could be somewhat less structurally robust than other parts of the caldera rim. The low point on the caldera rim (**Figure 2B**) is underlain by a block-rich breccia emplaced about 6–6.5 ka, that was associated with a debris-avalanche produced by dome disruption that preceded caldera collapse (Fierstein, and Hildreth, 2008). The "Big Breccia" deposit fills preexisting drainages and low areas and is one of the main deposits that holds in the lake (Fierstein, and Hildreth, 2008). The deposit is massive, unstratified, about 25 m thick, and contains numerous blocks 2–4 m in diameter. The deposit matrix consists of coarse sandy material that is iron-stained and somewhat indurated possibly as a result of iron cementation (Fierstein and Hildreth, 2008).

3.5 Mount Katmai

Mount Katmai is a compound stratovolcano, about 10 km in diameter, that is also located in Katmai National Park on the northeastern Alaska Peninsula (**Figure 1**). Mount

Katmai experienced catastrophic caldera collapse during the June 1912 Katmai-Novarupta eruption (Hildreth and Fierstein, 2012a). The caldera has an area of 9.4×10^6 m^2 and is partially occupied by a lake of about 5.4×10^6 m^2 in area. The low point on the caldera rim is at an elevation of 1,470 m and the lake surface has an elevation of about 1,285 m (**Supplementary Figure S5**). The estimated elevation of the caldera floor is about 995 m, indicating that the lake has a depth of 290 m (Hildreth and Fierstein, 2012a). The maximum depth of a crater-filling lake is about 470 m and the maximum volume of water the crater could hold is $1.5–3.5 \times 10^9$ m^3 (**Table 1**). Upwelling associated with hydrothermal activity on the floor of the lake was reported by Motyka (1978).

Multiple glaciers that resided on the Mount Katmai edifice were truncated by caldera collapse in 1912 (Hildreth and Fierstein, 2012a). Several of these glaciers persist today and occupy shallow glacial troughs on the edifice flanks. Runoff from snow and ice melt and precipitation probably controls the water balance of the lake as there are no perennial streams that flow into the caldera.

The rocks exposed in the walls of the caldera consist of bedded lavas of basalt to rhyodacite composition and a variety of phreatomagmatic fragmental deposits (Hildreth and Fierstein, 2012b). Alteration is common on parts of the caldera wall (**Supplementary Figure S5**) and the extent of alteration is locally intense enough to obscure primary depositional features such as along the east wall of the caldera where the caldera rim is at its lowest elevation (**Figure 6** of Hildreth and Fierstein, 2012b). A possible zone of weakness on the northeast wall of the caldera is indicated by numerous dikes oriented roughly northeast-southwest (Hildreth and Fierstein, 2003; Hildreth and Fierstein, 2012b).

3.6 Mount Mageik

Mount Mageik is one of the Katmai group volcanoes located in Katmai National Park in the northeastern part of the Alaska Peninsula (**Figure 1**). The volcano consists of a 2,165-m-high compound andesite-dacite stratovolcano that includes four overlapping cones that make up a broad edifice that covers about 80 km^2 (Hildreth et al., 2000). A small, elongated crater about 350 m in length on the northeast side of the central peak contains a shallow crater lake that is also the source of vigorous fumarolic activity (**Supplementary Figure S6**). The crater lake covers an area of about 8,600 m^2 and the crater is roughly 8.5×10^4 m^2 in area. The low point on the south crater rim is about 1925 m above sea level (**Supplementary Figure S6**). At this point the maximum potential depth of a crater-filling lake is about 35 m and the corresponding lake volume would be about $3–22 \times 10^5$ m^3 (**Table 1**). The crater resides in andesite-dacite lava flows of late Pleistocene–Holocene age (Hildreth and Fierstein, 2003). Photographs of the crater indicate extensive areas of hydrothermal alteration (**Supplementary Figure S6**) indicating that the crater walls could be susceptible to failure or erosion by water.

3.7 Mount Martin

Mount Martin is a small volcanic cone of Holocene age that consists of numerous overlapping lava flows of blocky dacite (Hildreth and Fierstein, 2003). The volcanic pile rests on a high ridge of Jurassic rocks that provides much of the relief of the volcano. Martin has an active hydrothermal system and numerous jetting fumaroles along the floor of its crater just beyond the margin of a small crater lake (**Supplementary Figure S7**). The Martin crater has an area of about 1.2×10^5 m^2, and the lake covers about 9,700 m^2. The maximum lake volume the crater could hold is about $1–5 \times 10^5$ m^3 (**Table 1**). The cone of Mount Martin consists primarily of andesite ejecta including scoria, agglutinate, and phreatomagmatic breccia (Hildreth and Fierstein, 2003). These deposits are exposed in the crater walls and exhibit variable alteration.

3.8 Mount Dana

Mount Dana is a small volcanic center with a central crater about 2 km in diameter, located northeast of Pavlof Bay on the southwestern Alaska Peninsula (**Figure 1**). Little is known about the geology of the volcano and its eruptive history. Pyroclastic-flow deposits emplaced about 3.8 ka and presumably associated with a large explosive eruption that could have formed the crater are exposed on the west flank of the edifice (Wilson et al., 1995).

The summit crater of Dana volcano has an area of about 2.7×10^6 m^2, and the crater lake covers about 5.8×10^5 m^2. Because the crater is breached on the southwest flank and there is an outlet stream that exiting the lake (**Supplementary Figure S8**), it is unlikely that the lake could get much larger unless the outlet became blocked by a landslide. The depth of the lake is unknown, but is probably on the order of 30–40 m based on visual estimates made during a field visit by the author in 2005. For a lake 40 m deep, the lake volume would be $2.3–2.6 \times 10^7$ m^3 (**Table 1**).

3.9 Mount Hague

Mount Hague is a prominent stratocone within Emmons Lake caldera on the southwestern Alaska Peninsula (**Figure 1**). Mount Hague consists of a twin-peaked basaltic-andesite to dacite stratovolcano about 5 km wide at the base and about 750 m high (**Supplementary Figure S9**). The flanks are largely snow- and ice-covered and scalloped by glacial erosion. The summit area is marked by two over-lapping circular craters, each about 400 m in diameter (**Supplementary Figure S9**). The rim of the northern crater reaches an elevation of 1,540 m above sea level but is cut by the southern crater, indicating the latter is younger. The southern crater is about 250 m deep, and a fumarole field is visible when the crater floor is exposed; however, by mid-summer the bottom of the crater is commonly covered by an ephemeral lake (**Supplementary Figure S9**). The low point on the crater rim is about 1,350 m and the crater floor is about 1,260 m, indicating a maximum potential lake depth of about 90 m. For a lake of this depth, the maximum volume is about $4.6–13 \times 10^6$ m^3 (**Table 1**).

3.10 Makushin Volcano

Makushin Volcano is a 2,036-m-high stratovolcano on Unalaska Island located 8 km west of Dutch Harbor and Unalaska, Alaska (**Figure 1**). The volcano has had at least 17 eruptive episodes since the 1700 s and erupted most recently in 1995 (McGimsey and Neal, 1995; Miller et al., 1998). The summit crater has an area of about 350,000 m^2 and is roughly 217 by 250 m in diameter (**Supplementary Figure S10**). The lake on the floor of the crater has an area of about 24,500 m^2 (**Supplementary Figure S10**). The crater was the source of minor eruptive activity in 1995 when a single eruptive burst generated an ash cloud that reached about 2,400 m above sea level and produced trace ash fallout on the upper part of the edifice (McGimsey and Neal, 1996).

The summit crater is surrounded by an extensive snow and ice field and there are multiple active fumaroles on the crater floor (Werner et al., 2020). The hydrothermal system at Makushin is active and likely driven by shallow magma beneath the summit region (Motyka, et al., 1988). Rock and pyroclastic deposits exposed in the walls of the crater are hydrothermally altered, indicating that the rock mass strength of the crater is likely compromised and could be susceptible to erosion or failure should a larger lake develop in the crater. The crater has a depth of about 100 m and thus the maximum volume of water the crater could hold is 4.2–19 × 10^5 m^3 (**Table 1**).

3.11 Tana Volcano

Tana volcano forms the eastern part of Chuginadak Island and is located east of Cleveland volcano (**Figure 1**). Little is known about the geology and eruptive history of the volcano. Photographs of the crater (**Supplementary Figure S11**) and studies of surficial deposits on the flanks of Tana (Persico et al., 2019) indicate that parts of the edifice are hydrothermally altered. Hot springs and active fumaroles on the flanks of the volcano are described in Werner et al. (2020). The crater on Tana has an area of about 7.7 × 10^5 m^2, and the crater lake covers about 2.1 × 10^5 m^2. The low point on the crater rim is about 780 m, only about 10 m above the modern lake level. The maximum possible volume of a crater lake is about 0.5–3.4 × 10^6 m^3 (**Table 1**).

3.12 Herbert Volcano

Herbert volcano on Herbert Island, is in the Islands of the Four Mountains area of the Aleutian Islands and is the western most volcano of this group of volcanic islands (**Figure 1**). Little is known about the geology and eruptive history of Herbert. The summit of the volcano is characterized by a circular 2.1 km diameter crater (or small caldera) that hosts a small lake that is about 5.7 × 10^5 m^2 in area (**Supplementary Figure S12**). The low point on the crater rim is about 840 m and this corresponds to a maximum potential lake area of about 1.9 × 10^6 m^2. The depth of the largest lake the crater could hold is about 220 m and the volume 1.8–4.2 × 10^8 m^3 (**Table 1**).

3.13 Korovin Volcano

Korovin is one of several stratovolcanoes on the northern part of Atka Island in the central Aleutian Islands (**Figure 1**). The village of Atka is 21 km south of the volcano. The Korovin summit edifice includes two craters, and the southern crater hosts the active vent and contains a small warm lake. Korovin has had minor episodes of phreatomagmatic eruptive activity in 2005, 1998, 1996, 1987, 1986, 1976, 1973, 1954, 1951, and 1907. Some of these eruptions generated small amounts of ash and lava flows of limited extent (Miller et al., 1998; McGimsey et al., 2003). The 1998 eruption produced an ash cloud that reached about 9 km above sea level. Fumaroles and warm mud springs are plentiful on the western and southern flanks of the volcano and overall the level of hydrothermal activity on and around the Korovin edifice is relatively high.

The south crater of the Korovin edifice has an area of about 3.7 × 10^7 m^2 and is partially occupied by a lake with an area of 1.6 × 10^4 m^2 (**Supplementary Figure S13**). The maximum depth of a crater filling lake is about 140 m and the maximum volume 2.3–3.6 × 10^7 m^3 (**Table 1**). The walls of the south crater consist of interbedded lava flows and pyroclastic deposits that do not appear significantly altered except at the base of the crater around the crater lake (**Supplementary Figure S13**).

3.14 Kasatochi Volcano

Kasatochi is a small, isolated island volcano in the east-central part of the Aleutian Arc (**Figure 1**). The volcano makes up all of Kasatochi Island and consists of a circular cone about 3 km in diameter with a lake-filled central crater (**Supplementary Figure S14**) that exhibited minor fumarolic activity in 2005 (McGimsey et al., 2008). Kasatochi experienced a 21-hour-long VEI 4 eruption on August 7–8, 2008 that was the only known historical eruption of the volcano (Waythomas et al., 2010a). As a result of the 2008 eruption, the summit crater was widened by several tens of meters and Kasatochi Island was covered with many tens of meters of pyroclastic debris and fine ash (Nye et al., 2017; Scott et al., 2010; Waythomas et al., 2010b). The Kasatochi summit crater has an area of about 1.5 × 10^6 m^2, and the crater lake has an area of 8 × 10^5 m^2 as determined from a November 22, 2020 WorldView-3, satellite image (**Table 1**). The crater lake had a depth of about 20 m when estimated in 2009 (Nye et al., 2017). The low point on the crater rim is about 160 m above sea level indicating that the maximum depth of the largest possible crater lake is roughly 180 m (**Supplementary Figure S14**). The area of the largest possible lake in the crater is about 1.3 × 10^6 m^2 and the volume about 2.2 × 10^8 m^3.

Geologic studies of Kasatochi following its 2008 eruption indicate that the walls of the crater consist of variable assemblages of bedded lavas and pyroclastic deposits (**Figure 7**, **Supplementary Figure S14**). The pyroclastic deposits on the west and south rims of the crater are loose and not well consolidated and are likely susceptible to erosion by water. The lava flows exposed beneath the low point on the crater rim are thin bedded with rubbly margins (Nye et al., 2017) and could be susceptible to piping should the crater lake increase in volume and approach the low point on the crater rim. Conduit-like, focused flow of water into the crater after the 2008 eruption (Waythomas et al., 2010a) indicates that parts of the crater walls could allow piping style drainage.

3.15 North Crater of Cerberus Volcano

The north crater of Cerberus volcano on Semisopochnoi Island (**Figure 1**) contains an ephemeral lake that was observed during recent periods of unrest in 2020-2021 at north crater. The crater is about 400 m in diameter and has an area of 1.5 × 10^7 m^2. Intermittent satellite observations since 2014, indicate that a small ephemeral lake is

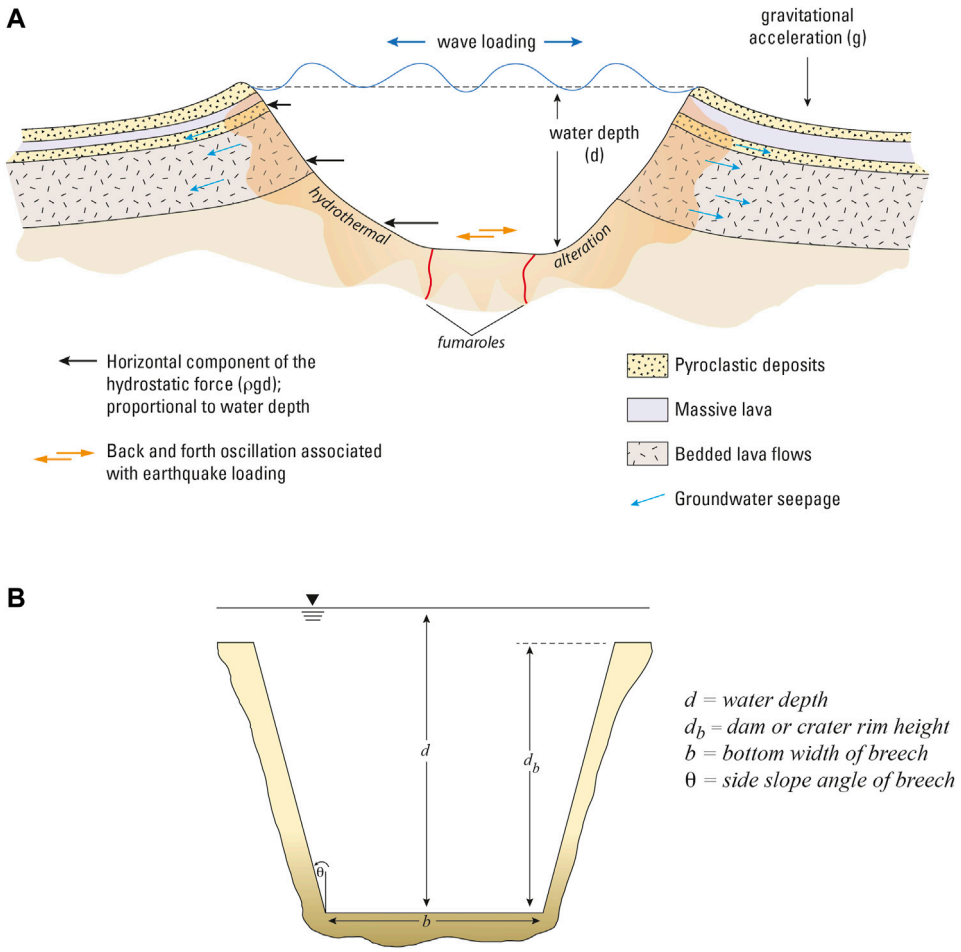

FIGURE 3 | Summary of forces and nomenclature for lake-filled volcanic craters at a typical stratocone. **(A)**. Generic cross section through a lake filled volcanic crater showing idealized stratigraphic elements, zone of hydrothermal alteration, and basic forces acting on crater walls. Fumaroles can occur on the crater walls as well as crater floors. The symbol ρ is water density. **(B)**. Trapezoidal breach and relevant geometric parameters.

sometimes present on the crater floor and likely develops in response to snowmelt runoff sometimes induced by unrest related geothermal heat flow and fumarolic activity within the upper edifice of the north cone. Although its size varies, the crater lake has an area of 6–9 × 10^3 m^3. The low point on the crater rim is about 750 m above sea level, and at this elevation the maximum area of a crater lake is 1×10^5 m^2. The maximum depth is about 120 m and thus the greatest volume of water the crater could hold is about 6–7 × 10^6 m^3 (**Table 1**).

The north cone is a basaltic-andesite edifice that consists of lava flows and pyroclastic deposits which are exposed in the walls of the crater (Coombs et al., 2018). None of these deposits appear altered, and the crater itself is steep and little modified (**Supplementary Figure S15**).

4 CRATER STABILITY AND SUSCEPTIBILITY TO FAILURE

The stability of lake-filled volcanic craters in Alaska is a key unknown in the assessment of plausible crater wall failures leading to water floods and associated water-saturated mass flows. The rocks and volcaniclastic deposits that make up many volcanic edifices may be structurally weak as a result of hydrothermal alteration (**Figure 3A**). The inconsistent nature of edifice stratigraphy, where loose, weak, pyroclastic deposits are interbedded with stronger materials such as lava flows also contributes to potential crater wall instability. Localized degradation of crater walls is indicated by accumulations of rockfall talus common on crater floors that is related to the structural integrity of the rocks and deposits that make up the crater. Many of the lake-filled volcanic craters in Alaska have steep internal slopes, include active hydrothermal systems, and exhibit at least surficial evidence of hydrothermal alteration. Some volcanic craters include thick deposits of tephra and pyroclastic density current deposits that are more susceptible to erosion than lava flows or welded spatter. This suggests that volcanic crater walls in Alaska possess some inherent instability.

From a hazard assessment perspective, volcanic craters and calderas are likely to be most susceptible to failure when the lakes they host are at or near capacity. In this state, crater rims are

TABLE 2 | Maximum volcanic crater slope angles, extent of surface alteration, and plausible mode of rim failure.

Volcano	Maximum inner crater wall slope angle, degrees	Hydrothermal alteration of crater walls	Active hydrothermal system present or not	Likely failure mode	Comments
Spurr summit	50–60	Yes. Type and extent not known	Ephemeral	Overtopping	Glacier ice and snow on crater rim. Abundant ice and snow on flanks of summit cone. Lack of obvious melting since about 2010 indicates hydrothermal activity greatly diminished or stopped
Crater Peak	50–60	None apparent	Ephemeral	Overtopping	Crater Peak cone consists primarily of stacks of lava flows with only minor layers of pyroclastic debris
Douglas	40–50	Yes. Type and extent not known	Active	Overtopping	Glacier ice and snow on crater rim. Abundant ice and snow on flanks of summit cone
Kaguyak	30–50	Minor. Type and extent not known	Inactive	Overtopping Piping?	Loose, unconsolidated material occupies lowest terrain on crater rim
Katmai	40–60	Yes. Type and extent not known	Inactive	Overtopping	Some bubbling observed but no robust hydrothermal activity reported. Local slope failures could displace water possibly resulting in overtopping
Mageik	30–45	Yes. Type and extent not known	Active	Overtopping	Crater walls consist primarily of altered lava flows and minor pyroclastic and tephra deposits
Martin	40–60	Yes. Type and extent not known	Active	Overtopping	
Chiginagak	30–50	Yes. Type and extent not known	Ephemeral	Subglacial tunnel	Low point on crater rim mantled by glacier ice forming an ice dam
Dana	30–50	None apparent	Inactive	Overtopping	Outlet stream drains crater lake; a landslide would have to block the channel for a larger lake to form
Hague	30–50	Yes. Type and extent not known	Ephemeral	Overtopping	
Makushin	40–60	Yes. Type and extent not known	Active	Overtopping	Glacier ice and snow on crater rim. Abundant ice and snow on flanks of summit cone
Tana	30–50	Yes. Type and extent not known	Inactive	Overtopping	
Herbert	30–50	Minor. Type and extent not known	Inactive	Overtopping	Little known about the geology of the crater
Korovin	40–60	Yes. Type and extent not known	Active	Overtopping	
Kasatochi	40–60	Yes. Type and extent not known	Generally inactive	Overtopping	Hydrothermal activity increased prior to the 2008 eruption but observations were sporadic
North crater, Cerberus	40–60	None apparent	Ephemeral	Overtopping	Satellite observations indicate that the lake is ephemeral

analogous to other types of natural or constructed dams (such as landslide dams, moraine dams, earth-fill dams, concrete dams, or embankment dams) and can be evaluated as such. The most common mechanism for failure of natural and constructed dams is by overtopping and roughly 90% of landslide dams fail by this process (Costa and Schuster, 1988). Constructed dams of various types also fail predominantly by overtopping but also by piping, seepage, and as a result of foundation defects (Costa, 1985; Foster et al., 2000). Overtopping failures develop from water flowing over the dam crest and subsequent erosion of the dam face. Commonly, water flow over the dam crest results in headward erosion of the dam face until the dam crest is breached, allowing more water to escape resulting in further erosion of the breach. Water seepage through the dam may accelerate the process, especially if groundwater piping develops and some natural dams fail primarily as a result of piping (Costa and Schuster, 1988). For a static condition, with no external stresses applied to the crater wall or lake, the hydrostatic pressure associated with the crater lake can result in the development of saturated conditions within all or part of the crater wall materials. If the crater wall materials are saturated, they should exhibit a decrease in shear strength such that the factor of safety (F_s) is reduced.

Eruptive activity from underwater vents could lead to forceable ejection of water or waves sufficient to overtop crater rim dams. The combined effects of eruptive activity and associated water displacement may enhance erosion of the dam and lead to breaching. In contrast, slow spillover of water associated with hydrologic changes of the lake basin such as rapid snow or ice melt or extreme rainfall (Yang et al., 2005) could also lead to eventual dam breach.

Preliminary stability information for the 16 lake-filled craters evaluated in this study is given in **Table 2**. The steepest parts of the crater walls are in the range of 30–60° and all but Crater Peak and Dana exhibit some outward evidence for hydrothermal alteration. Five of the craters have active hydrothermal systems, six have ephemeral hydrothermal systems, and five have no apparent modern hydrothermal activity (**Table 2**). Hydrothermally altered volcanic edifices have an increased susceptibility to gravitational failure because of the general loss of rock mass strength associated with alteration (Watters, et al.,

2000; Reid et al., 2001; Finn et al., 2018). Crater wall collapse resulting from hydrothermal alteration could be triggered by intense seismic shaking, eruptive activity, or increases in hydrostatic pressure and wall loading associated with the crater lakes if they were at or near full crater capacity (**Figure 3A**).

4.1 Seismic Effects on Volcanic Crater Lakes

Assuming that it is possible for the crater lakes to increase in volume and approach spillover, an important stability concern are the hydrodynamic pressures on the crater walls induced by seismic shaking of the crater lake. Large-magnitude earthquakes (>M7) are common in the Aleutian Arc with one or more occurring almost annually (Sykes et al., 1981) and intense seismic shaking is a well-known mechanism for inducing failure of natural dams (Costa and Schuster, 1988). The magnitude of hydrodynamic pressure depends on the frequency-magnitude characteristics of the seismic load and the material properties of the crater walls. In addition, the seismic shaking of a lake-filled volcanic crater can induce changes in pore-fluid pressure within the crater walls and an associated reduction in shear strength. Volcanic craters that are hydrothermally altered or contain layers that transmit groundwater could be particularly susceptible to failure under seismic loading. In a study of the seismic response of earth-fill dams, Gazetas (1987) showed that ground accelerations are higher near the crest of the dam, suggesting that for lake-filled volcanic craters filled to near capacity, seismic accelerations may be sufficient to cause overtopping and water spillover.

The maximum hydrodynamic pressure ($p_{\max}$) occurs at the base of the crater wall dam and can be expressed as:

$$p_{max} = 0.7 a_c \gamma_w h \tag{1}$$

where a_c is the acceleration coefficient ($a_c = \frac{a_0}{g}$ where a_0 is the maximum value of the horizontal acceleration and g is gravitational acceleration), γ_w is the unit weight of water, and h is the depth of the lake at the crater wall (Pelecanos et al., 2013). This expression is valid for a dam with a vertical lake-side profile. If the internal crater wall is inclined, the hydrodynamic pressure $p_{(y)}$ is expressed as:

$$p_{(y)} = C_p a_c \gamma_w h \tag{2}$$

where C_p is a pressure coefficient (determined analytically, Chwang and Housner, 1978; Chwang, 1978), a_c is the acceleration coefficient, γ_w is the unit weight of water, and h is the depth of the lake (Pelecanos et al., 2013).

Earthquake induced forces on the reservoir-dam system were evaluated by Chwang and Housner (1978). Their analysis concluded that for dams with lake side facing slopes of 0–90°, the total horizontal force on the dam (F_x) is:

$$F_x = C_x \rho a_0 h^2 \tag{3}$$

where C_x is a force coefficient (~0.5), ρ is water density, and a_0 and h^2 are as defined above. Peak ground accelerations in the central-western Aleutian Arc associated with large megathrust earthquakes are roughly in the range of 4–8 m/s^2 (Wesson et al., 2007). Using these values for a_0 in the above expression and 1,000 kg/m^3 for ρ, the estimated maximum force on the crater wall dam for a lake 50 m deep is 1–2 × 10^5 N. For a lake 100 m deep, F_x is 2–4 × 10^5 N. If it is assumed that peak ground acceleration occurs in a largely bidirectional, back and forth manner, only those parts of the crater wall in the domain of motion would be subject to the maximum forces. Using a 200 m long sector of a generic crater and crater lake depths of 50 and 100 m, the above estimated forces would generate maximum crater wall pressures of only 10–40 Pa which are very low and probably not significant enough to cause failure of the crater wall by this mechanism alone.

Seismic shaking of lake-filled volcanic craters could result in liquefaction of strata within the crater walls which could be sufficient to cause crater rim failure. Several tailings dams have failed by this process (Lyu et al., 2019) and where significant portions of volcanic crater walls are composed of relatively loose, unconsolidated or hydrothermally altered material, seismically induced liquefaction could be a concern. The duration and peak ground accelerations associated with large earthquakes also can result in back-and-forth water oscillations known as seiches (McGarr and Vorhis, 1968). Seismic seiches at volcanic lakes are not widely known, but the few examples described in the literature indicate that seiches can be hazardous (Moore et al., 1966; Newhall and Dzurisin, 1988) and could be large enough to overtop crater rims which may lead to water erosion and possible dam failure.

4.2 Volcanic Crater Lake Hydrology

Although it is beyond the scope of this paper to make a quantitative assessment of crater lake hydrology at each location discussed, some general commentary on the hydrologic setting of the Alaska crater lakes is warranted and provides some insight on the potential for changes in the water balance of the lakes. The primary hydrologic inputs are precipitation (snow, meltwater, rainfall; W_p), groundwater (W_g), and water from shallow magmatic sources (W_v). These inputs are affected by evaporation (W_e) and water outflow, either as direct open-channel flow (W_o), groundwater seepage (W_{gw}), or both, such that $W_p + W_g + W_v = W_e + W_o + W_{gw}$ which is a general statement for the water balance of the lake (Pasternack and Varekamp, 1997; Rouwet et al., 2004). None of these variables are known with any degree of certainty for the Alaska crater lake examples discussed here. The Alaska volcanic craters are situated at the summit of their respective volcanic edifices and the crater itself defines the hydrologic catchment. Of the 16 volcanic craters examined in this study, nine are on volcanoes with significant amounts of glacier ice (>1 km^2; GLIMS Consortium, 2005) and the remaining six craters are in areas that receive seasonal snow (typically September–April) that can exceed several meters depth (Brown et al., 2003; https://www.weather.gov/aprfc/Snow_Depth). The volume of glacier ice on volcanoes in Alaska has been measured only at a few locations. At Mount Spurr, about 67 km^3 of glacier ice and perennial snow was present on the edifice when measured in 1981 (March et al., 1997) indicating ice

volumes at similar glaciated stratovolcanoes in Alaska are significant (Waythomas, 2015). Thus, a main hydrologic input, snow and glacier ice, is present at all locations in ample amounts. An example discussed in *Lahars* below, shows that an increase in the thermal output at an ice and snow-clad volcanic crater (Mount Spurr) could be sufficient to cause melting and increase the water input to the crater lake. An increase in heat flux at Chiginagak volcano also led to significant melting and an increase in the volume of the crater lake eventually resulting in catastrophic lake drainage (Schaefer et al., 2008).

All volcanic crater locations receive significant precipitation and annual amounts of >1 m (water equivalent) are not uncommon (Stafford et al., 2000) although long-term weather records in the study region are available only at a few localities at sea level. If a generic volcanic crater with an area of 1×10^5 m^2 receives 1 m of snow accumulation, the approximate snow-water equivalent (SWE) is about 5×10^4 m^3 of water if the SWE of 1 m of snow is about 50 cm water (Sturm et al., 2010). Thus, snowfall could represent a significant input to the Alaska crater lakes although some of this water will be lost to evaporation and groundwater seepage. These components of the water balance are difficult to estimate and although various springs have been observed (Motyka et al., 1993; Evans et al., 2015), little is known about water flux or the state of groundwater at any of the volcanic craters discussed here.

Systematic measurements of water levels in the Alaska crater lakes have not been accomplished, although opportunistic observations, photographs, and satellite data have provided a general sense of the presence and extent of lakes in some locations as described in *Crater Lakes in Alaska* above. Evidence of significant changes in water levels have been noted at Mount Spurr, Crater Peak, Chiginagak, Korovin, and north crater on Cerberus volcano. The summit craters at Mount Spurr and Chiginagak, and possibly Korovin and north crater have been affected by changes in the thermal output of the volcano. A lake was present at Crater Peak prior to the eruptive activity in 1992 and has not reappeared since suggesting that it too may have been a result of an increase in heat flow resulting in local snow and ice melt. Water level observations of Katmai Lake were made in the 1970s and from July 5, 1975, to August 20, 1977, the water level increased by about 6.5 m or an average rate of 3 m/yr (Motyka, 1978). Apparently, Katmai Lake drained sometime between 1919 and 1923 (Fenner, 1930). None of the other cater lakes exhibit any obvious evidence for fluctuations in lake level but it is clear from the few available observations that significant changes in water volume can occur.

5 CRATER RIM OVERTOPPING, BREACH FORMATION, AND PEAK FLOOD DISCHARGE

Assuming that sufficient water can be made to flow over the crater rim to initiate breach formation at the locations considered here, the maximum discharge at the breach can be evaluated using the same techniques for evaluation of breach formation at generic earth-fill dams (Fread, 1996; Walder and O'Connor, 1997; Froehlich, 2008). Given that it would be difficult to specify all the conditions of breaching at the lake-filled craters described here, the goal is to provide first order estimates of the maximum possible peak discharge at the breach from a worst-case scenario perspective. To accomplish this, the method for predicting peak discharge by dam breaching described in Walder and O'Connor (1997) is used.

The physically based model of dam-breach formation described in Walder and O'Connor (1997) makes use of the well-known kinematics of breach formation and the hydraulics of flow through a breach of known shape (typically trapezoidal, **Figure 3B**; Henderson, 1966). This approach provides estimates of peak discharge at the breach that are dependent on the volume of impounded water, breach erosion rate and shape, and lake hypsometry. The discharge estimation technique makes use of a functional relationship between dimensionless peak discharge (Q_p^*) and a dimensionless parameter η ($\eta = kV_0/g^{1/2}d^{7/2}$), where k is the breach erosion rate, V_0 is the initial volume of the lake, g is gravitational acceleration, and d is the drop in lake level. The dimensionless peak discharge is expressed as

$$Q_p^* = \alpha\eta^\beta \tag{4}$$

where α and β are dimensionless coefficients that depend on the width-depth ratio of the breach, the side slope angles of the breach, and crater-lake hypsometry (Walder and O'Connor, 1997).

Assuming that a crater-rim breach forms rapidly to the full depth of the lake and the shape remains relatively fixed throughout the event (MacDonald and Langridge-Monopolis, 1984; Singh et al., 1988; Walder and O'Connor, 1997), the analysis of peak outflow can be simplified such that maximum peak discharge at the breach (Q_p) can be estimated as follows:

$$Q_p = 1.94 g^{1/2} d^{5/2} \left(\frac{D_c}{d}\right)^{3/4} \tag{5}$$

where D_c is the height of the dam crest relative to the dam base. For a worst-case scenario where the breach develops to the full depth of the lake at the breach (d), $d = D_c$. This reduces the expression for Q_p to:

$$Q_p = 1.94 g^{1/2} d^{5/2} \tag{6}$$

and is applicable in situations of rapid breach formation where $\eta \gg 1$. For cases where breach development occurs slowly, and $\eta < 1$, the maximum peak discharge is expressed as:

$$Q_p = 1.51\left(g^{\frac{1}{2}} d^{\frac{5}{2}}\right) \cdot 0.06\left(kV_0/d\right)^{0.94} \tag{7}$$

Breach formation is assumed to occur at a constant rate k through the full depth of the lake at the breach. Values of $k = 1$, 10, and 100 m/h provide estimates of slow to fast breach formation. Studies of breach development during dam failures indicate that the final breach shape is almost always trapezoidal (MacDonald and Langridge-Monopolis, 1984; Singh et al., 1988). Assuming that crater lake breaches are

TABLE 3 | Peak discharge estimates for hypothetical crater-lake dam failure floods at selected Alaska volcanoes assuming maximum initial crater lake volume. 1) calculated from: $Q_p = (c_1 r + c_2 cot\theta) g^{0.5} d^{2.5}$ 2) calculated from: $Q_p = 1.94 g^{1/2} d^{5/2}$ (3, 4, 5) calculated from: $Q_p = 1.51 (g^{\frac{1}{2}} d^{\frac{5}{2}})^{0.06} (kV_0/d)^{0.94}$ where k = 1, 10, and 100 m/h.

Volcano	Maximum crater lake volume V_0, in m^3	(1) Maximum peak discharge, Q_p in m^3/s (trapezoidal breach)	(2) Maximum peak discharge, Q_p in m^3/s ($\eta \gg 1$)	(3) Maximum peak discharge, Q_p in m^3/s (k = 1 m/h)	(4) Maximum peak discharge, Q_p in m^3/s (k = 10 m/h)	(5) Maximum peak discharge, Q_p in m^3/s (k = 100 m/h)
Mt. Spurr summit	9.7×10^6	5.16×10^5	1.41×10^6	47	4.1×10^2	3.6×10^3
Crater Peak	1.4×10^7	2.25×10^4	6.15×10^4	29	2.6×10^2	2.2×10^4
Douglas	1×10^6	2.25×10^4	6.15×10^4	17	1.5×10^2	1.3×10^3
Kaguyak	9×10^8	6.13×10^5	1.67×10^6	3.3×10^3	2.8×10^4	2.5×10^5
Katmai	3.5×10^9	3.19×10^6	8.7×10^6	$3.4\ 10^3$	2.9×10^4	2.6×10^5
Mageik	2.2×10^6	1.61×10^4	4.4×10^4	6	54	4.7×10^2
Martin	5.1×10^6	3.93×10^4	1.07×10^5	14	1.2×10^2	1×10^3
Chiginagak	3.8×10^6	2.25×10^4	6.15×10^4	59	5.1×10^2	4.5×10^3
Dana	2.6×10^7	2.25×10^4	6.15×10^4	3.6×10^2	3.1×10^3	2.7×10^4
Hague	1.3×10^7	1.71×10^5	4.67×10^5	37	3.2×10^2	2.8×10^3
Makushin	3.5×10^7	2.23×10^5	6.07×10^5	15	1.3×10^2	1.1×10^4
Tana	3.4×10^6	3.98×10^3	1.09×10^4	92	8×10^2	7×10^3
Herbert	4.2×10^8	1.6×10^6	4.36×10^6	1×10^3	9.4×10^3	8.2×10^4
Korovin	3.6×10^7	5.16×10^5	1.41×10^6	1.2×10^2	1×10^3	9.1×10^3
Kasatochi	2.2×10^8	9.67×10^5	2.64×10^6	7.5×10^2	6.5×10^3	5.7×10^4
N. crater, Cerberus	1.3×10^7	3.51×10^5	9.58×10^5	47	4×10^2	3.5×10^3

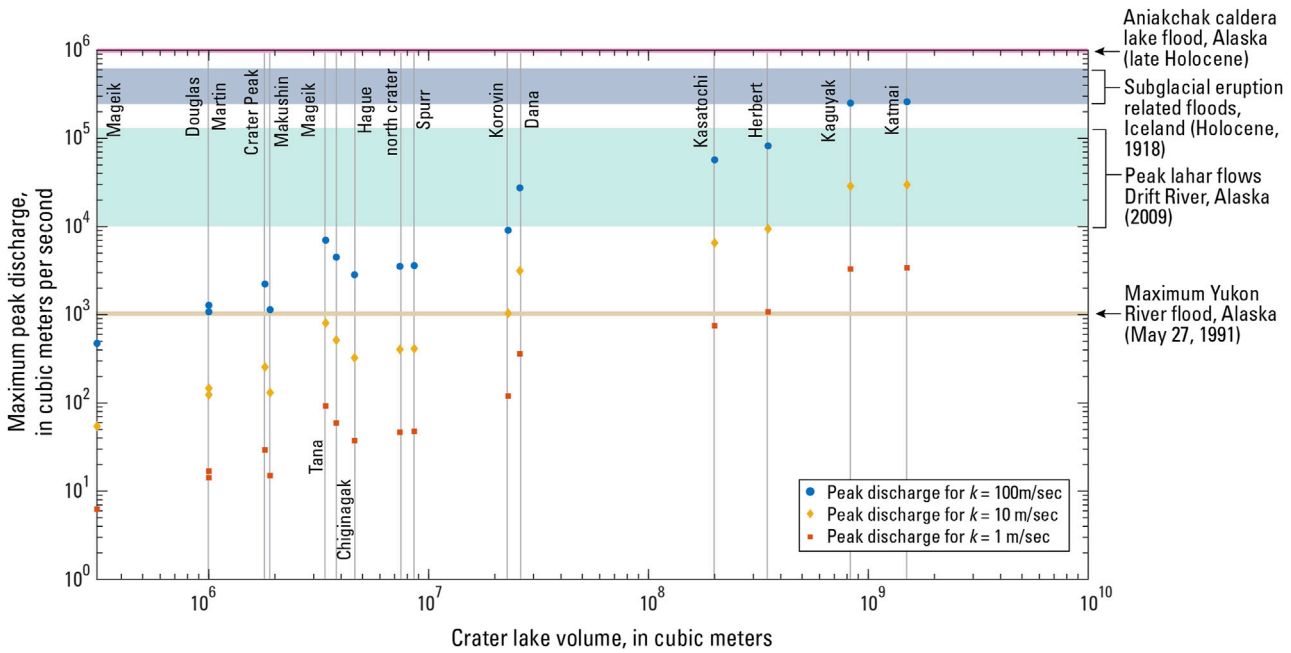

FIGURE 4 | Comparison of maximum peak discharge from hypothetical crater-lake floods in Alaska to other large flows. Peak discharge of Alaska crater-lake floods for breach erosion rates of 1, 10, and 100 m/s estimated with **Eq. 7**. Aniakchak peak discharge estimate from Waythomas et al., 1996; subglacial eruption related flood and Yukon River discharge estimates from O'Connor and Costa, 2004; Drift River lahar discharge estimates from Waythomas et al., 2013.

also trapezoidal in shape, the maximum peak discharge at the breach can be expressed as a relation among Q_p, breach shape and water depth:

$$Q_p = (c_1 b + c_2 H cot\theta) g^{0.5} H^{1.5} \quad (8)$$

where b is the bottom width of the breach, θ is the angle of the breach side slope, c_1 and c_2 are geometric constants ($c_1 = 0.544, c_2 = 0.405$), and H is the water depth of the lake above the base of the breach (Waythomas et al., 1996). If the breach shape remains geometrically similar throughout its formation, the geometric variables c_1, c_2, b, and θ are constants. When the time of breach formation (t) is $\geq d/k$, $b = rd$ where the b/d ratio is ~2.5 (Singh et al., 1988; Waythomas et al., 1996).

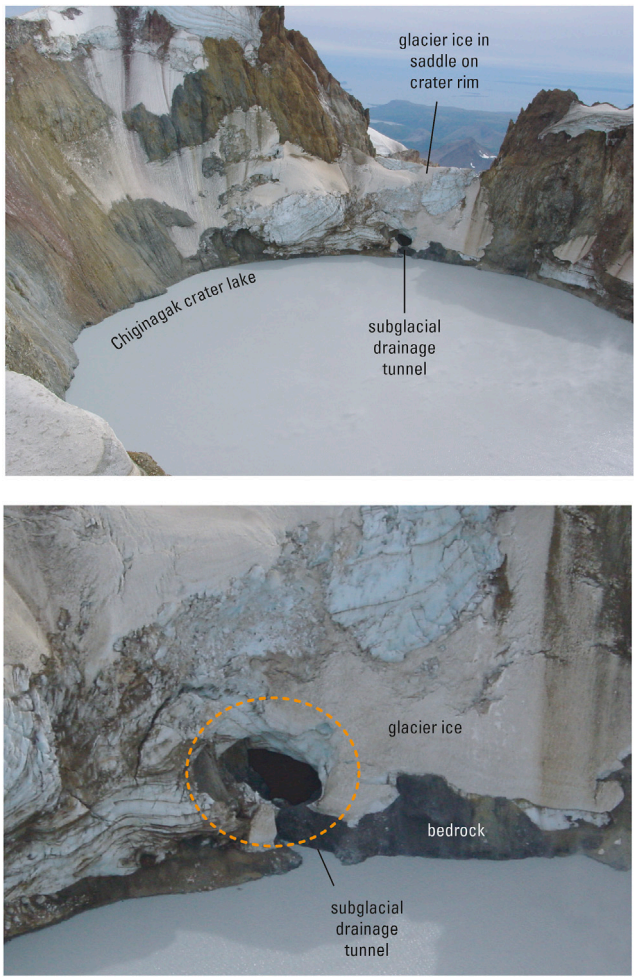

FIGURE 5 | Photographs of subglacial tunnel and site of May 2005 lake drainage event on the rim of the Chiginagak crater. Photographs by R.G. McGimsey, AVO, August 21, 2006.

Lake depth is related to lake volume by the following hypsometric relation:

$$\left(\frac{V}{V_0}\right) = \left(\frac{h_l}{h_0}\right)^p \tag{9}$$

where h_l is the water depth at lake volume V, and V_0 and h_0 are initial values of lake volume and water depth ($h_0 = d$). The exponent p is specific to each lake basin; for long, narrow basins $p \sim 1$ and for circular basins, $p \sim 3$, thus for the crater lakes and calderas examined here, $p = 3$ is used.

The change in water depth at the breach (H) with time (t) is:

$$\frac{dH}{dt} = -\left(\frac{D^p}{pV_0}\right) g^{0.5} H^{2.5-p} (c_1 rD + c_2 H cot\theta) \tag{10}$$

and the maximum theoretical peak discharge for an instantaneously formed breach to the maximum depth of the lake at the breach is:

$$Q_p = (c_1 r + c_2 cot\theta) g^{0.5} d^{2.5} \tag{11}$$

5.1 Discussion of Peak Discharge Estimates

The results of peak discharge estimates for water floods produced by crater wall collapse are given in **Table 3**. The estimates are based on maximum peak discharge associated with a fully formed trapezoidal breach calculated with **Eq. 11**, maximum peak discharge for rapid breach formation calculated with **Eq. 6**, and maximum peak discharge calculated with **Eq. 7** where breach erosion rate k is set to 1, 10, and 100 m/h.

The largest peak discharge values result from application of **Eq. 6** where breach formation is essentially instantaneous. These values are an upper bound on peak discharge and thus may be taken as representing the worst-case condition. The peak discharge values obtained from **Eq. 6** are similar to those resulting from **Eq. 11** where a trapezoidal-shaped breach is assumed throughout each crater rim failure flood event.

Values for maximum peak discharge determined from **Eq. 7** are shown in **Figure 4**. Also shown in **Figure 4** are the maximum peak discharges for other large outburst floods and lahars in Alaska and Iceland. Flood magnitudes associated with water-filled volcanic craters in Alaska are comparable to these volcanogenic flows and river floods and this highlights the potential significance of the Alaska examples.

Variable breach erosion rates in **Eq. 7** yield much smaller values for maximum peak discharge compared to estimates based on nearly instantaneous breach formation (**Table 3**). Although it is difficult to accurately determine the erosion rate of a crater rim a priori, the discharge estimates in **Table 3** indicate the strong dependence between erosion rate and peak discharge. There may be situations where it is possible to reasonably estimate the breach erosion rate and thus application of **Eq. 7** in these situations would be warranted.

6 CRATER LAKE FLOODS ASSOCIATED WITH GLACIER ICE DAMS

Most of the crater lakes evaluated here do not involve glacier ice as a component of the natural dam. The three exceptions are Mount Spurr, Douglas volcano and Mount Chiginagak (**Supplementary Figures S1,3** and **Figure 5**). In these two cases, glacier ice covers a significant part of the crater wall and is either known (Chiginagak) or suspected (Spurr, Douglas) to play a role in the development of floods from the associated lake-filled crater.

At Douglas volcano, a significant portion of the crater wall is covered by glacier ice of unknown geometry. It may be that glacier ice simply drapes the crater rim, although photographs of the crater indicate that glacier ice fills several of the low areas along the rim (**Supplementary Figure S3**). If the crater lake were to increase in volume, the ice may melt, exposing the crater wall, or the ice could lend stability to the rim and make it less susceptible to erosion or failure if the ice cover is thick (>100 m). If the glacier ice is a part of the crater rim, rising lake levels could destabilize the ice when the impounded water became deep enough to float or

TABLE 4 | Expected eruption characteristics in relation to crater lake water supply assuming sustained eruption through lake (Modified from Wohletz et al., 2009).

Water supply	Eruption characteristics	Volcanic cloud height	Main eruptive products
Unlimited	• Surtseyan jets • Base surges • Wet fallout	0.3–1.5 km	• Fine-grained surge deposits • Ballistic particles • Fine-coarse ash and lapilli
Available but not unlimited	• Violent magma-water interactions • Phreatoplinian eruption columns • Column collapse pyroclastic density currents	20–50 km	• Abundant fine ash • Pyroclastic mass-flow deposits • Extensive ash fallout

thermally erode the glacier dam (Björnsson, 1974; Nye, 1976). In this case, flow under the ice could eventually lead to the formation of a subglacial channel that would increase in size roughly proportional to the volume and duration of exiting lake water (Clarke, 1982). If glacier ice makes up a significant part of the crater wall, wholesale failure of the ice would be analogous to rapid breach formation as discussed in the previous section.

Lakes impounded by glaciers pose a well-known flood hazard and are often described as glacier outburst floods or jökulhlaups (Björnsson, 1974; Clague and O'Connor, 2021). For situations where water drainage occurs through a subglacial tunnel, peak discharge (Q_p) can be estimated using an empirical relation between Q_p and lake volume (V) (Walder and Costa, 1996):

$$Q_p = 46V^{0.66} \quad (12)$$

This equation provides first-order estimates of peak discharge for subglacial tunnel drainage but is less analytical than the method described in Clarke (1982) where lake temperature and rate of tunnel closure are incorporated into numerical expressions for Q_p. For the May 2005 crater lake flood at Chiginagak, the lake volume (V) drained was estimated at 3.8×10^6 m^3 (Schaefer et al., 2008). Application of **equation 12** yields $Q_p = 111$ m^3/s. At Chiginagak, elevated water surface temperatures of about 40°C were measured in the crater lake with a Forward Looking Infrared camera (FLIR) about 4 months after the May 2005 crater lake flood (Schaefer et al., 2008). This indicates that lake water temperature could have been of this magnitude when the flood occurred and suggests that the thermal energy of the lake likely influenced tunnel drainage at the base of the ice dam (**Figure 5**) and the Q_p estimate based on **Eq. 12** is likely a minimum value.

7 HAZARDS AND CONSEQUENCES OF ERUPTIONS THROUGH CRATER LAKES IN ALASKA

Of the sixteen volcanoes evaluated here, only six of them have had documented eruptive activity in the past 200-300 years (**Table 1**). However, all sixteen volcanoes have been active during mid–late Holocene time. Thus, it is not unreasonable to consider likely eruptive styles and hazards that are a consequence of future eruptions involving lake-filled craters and calderas addressed in this study. In addition to catastrophic crater rim failure floods described above that could occur during eruptive activity or not, other important hazards are a direct consequence of magma-water interaction influenced by significant volumes of water positioned above potentially active vents. Estimates of the maximum crater lake water depth at the point of spillover range from 10 to 470 m (**Table 1**). These water depths are generally considered shallow and would not exert significant hydrostatic pressure on rising magma to effect volatile exsolution such that explosive activity would be inhibited (Cas and Giordano, 2014). Thus, depending on the volatile content of the erupting magma, the lakes should have no significant effect on the explosiveness of potential eruptions assuming no direct magma-water interaction.

Magma-water interaction in the context of crater lakes can include a range of eruptive styles (**Table 4**), from non-explosive lava effusion to violent explosions associated with magma-water mixing (Kokelaar, 1986; Wohletz et al., 2009). Mafic eruptions involving crater lakes where the supply of water is essentially unlimited are typically Surtseyan style eruptions (Kokelaar, 1983; Németh et al., 2006). In cases where the eruptive conditions promote dynamic interaction of water and magma such that a significant vapor-phase component results, very violent phreatoplinian activity can occur. Both Surtseyan and phreatoplinian activity could generate hazardous phenomena (**Table 4**; Mastin and Witter, 2000; Manville, 2015) that would be significant to areas within 5–10 km of the erupting volcano and ash fallout could affect areas well beyond this range. Among the main outcomes of eruptive activity at the crater and caldera lakes evaluated here are explosive displacement of water, lahars, and base surges. These outcomes are discussed briefly below.

7.1 Explosive Displacement of Water

Expulsion of water beyond crater rims could occur during larger eruptions involving substantial amounts of volatile-rich magma, generally VEI 3 or larger, but possible for eruptions as small as VEI 1 (Mastin and Witter, 2000; Rouwet and Morrissey, 2015). Explosive displacement of water from crater lakes can take on several forms from small seiche-like or splash displacements that may or may not overtop the crater rim such as those that occurred during the initial unrest at Karymskoye Lake, Kamchatka in 1996 (Belousov and Belousova, 2009) and at Ruapehu volcano, New Zealand in 1995 (Lecointre et al., 2004; Kilgour et al., 2010) to wholesale evacuation of the entire crater lake. A numerical modeling study by Morrissey et al. (2010) indicated that if crater lake water depth is > 90 m and eruption pressures are <10 MPa, subaqueous jetting capable of breaching the water surface is unlikely to occur, whereas in situations where the eruption pressure is > 10 MPa, explosive jetting through the

FIGURE 6 | Photographs of Kasatochi crater lake, before **(A)** and after **(B,C)** the August 7, 2008, VEI 4 eruption. **(A)**. View across Kasatochi crater lake to the north, August 6, 2008. Photo by C. Ford, US Fish and Wildlife Service. **(B)**. Interior of Kasatochi crater and small, shallow lake on the crater floor, August 22, 2008, about 2 weeks after the 2008 eruption. View is toward the east. Photo by R. Buchheit, US Fish and Wildlife Service. **(C)**. Panorama of northern, eastern, and southern part of Kasatochi crater, taken from crater rim, August 10, 2010. Photo by J. Williams, US Fish and Wildlife Service.

water column and displacement of water can occur. Given these approximate constraints, physical disruption of crater lakes in Alaska should be expected during future eruptions should they occur at the volcanoes discussed.

7.1.1 Alaska Examples

Complete evacuation of a crater lake occurred during the 2008 eruption of Kasatochi volcano (**Figure 6**) and resulted in some interesting and possibly diagnostic deposits (**Figure 7**). Kasatochi as described previously has a summit-defining crater that hosts a lake that today is about 8.4×10^5 m^2 and has a volume of about 1.7×10^7 m^3. Although the pre-2008 lake was slightly smaller, the volume was likely on the order of 10^7 m^3 (**Figure 6**). This volume of water was explosively discharged from the crater during the early phase of the 2008 Kasatochi eruption (Waythomas et al., 2010a; Scott et al., 2010). Although not widespread on Kasatochi Island, the first of the 2008 eruptive deposits to accumulate were massive grey muddy tephra deposits and multiple beds of pumice rich coarse ash and mud that collectively are up to 50 cm thick. When freshly exposed by shovel, these deposits oxidize rapidly and take on a yellow-brown-gray color indicating that the muddy components were probably chemically reduced when deposited (Scott et al., 2010). The pH of

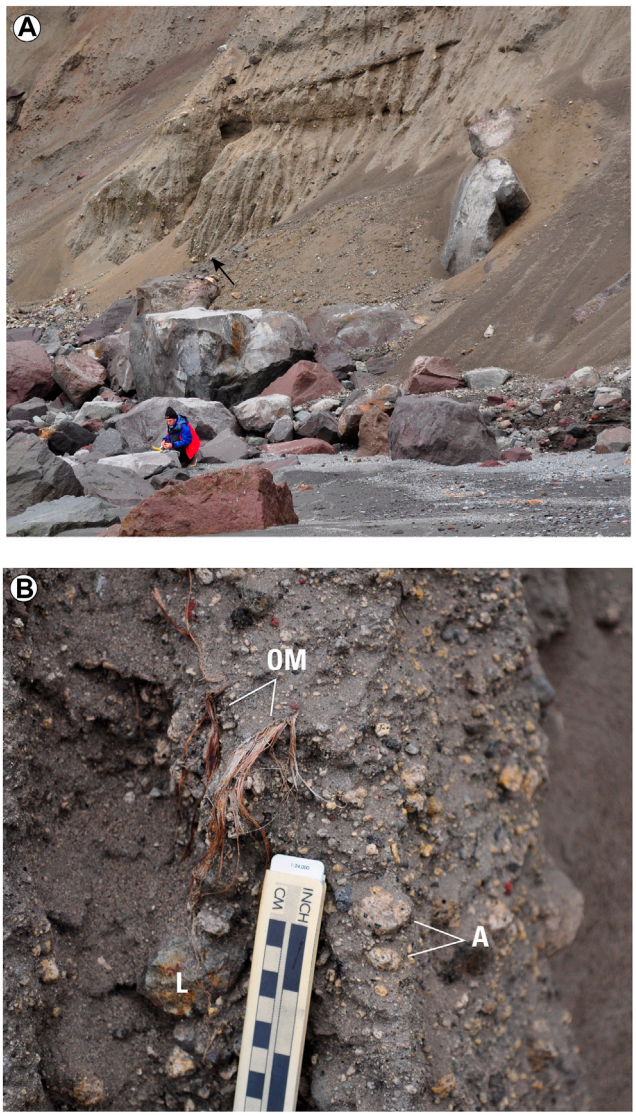

FIGURE 7 | Basal pyroclastic-flow deposits of the 2008 Kasatochi eruption, June 14, 2009. Both photos by C. Waythomas, AVO. **(A)**. Typical outcrop of lithic-rich pyroclastic-flow deposits on west side of Kasatochi Island. These deposits make up the first sequence of pyroclastic-flow deposits emplaced during the early part of the 2008 Kasatochi eruption. Arrow locates area of photo shown in **(B)**. Note person for scale in lower left. **(B)**. Close up view of pyroclastic-flow deposits containing unburned organic matter (OM), juvenile andesite (A) and lithic clasts (L). Organic matter like this is dispersed throughout the lower 1–2 m of the pyroclastic-flow deposits.

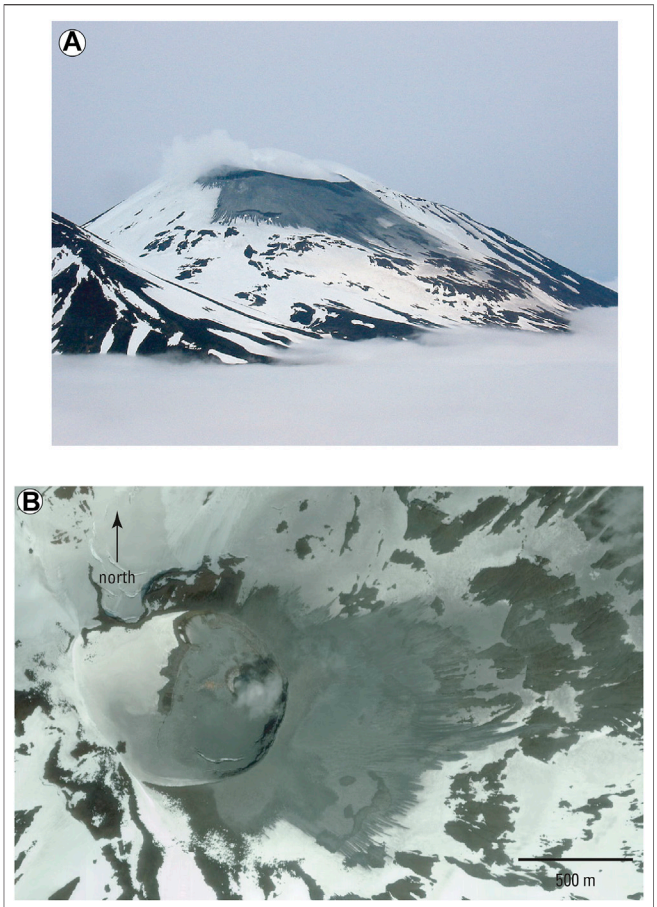

FIGURE 8 | Views of wet eruptive deposits on upper east flank of the south crater at Korovin volcano. **(A)**. Oblique photograph of Korovin south crater, July 1, 2004. Photo by T. Plucinski, AVO. **(B)**. True color Ikonos satellite image of the summit crater of Korovin volcano, July 4, 2004. Grey-colored ash and mass-flow deposit extends about 1 km beyond crater rim. A small lake that is typically present in the inner crater is absent in this image and was likely removed by the small eruption that produced the deposits evident on the east flank of the crater.

these deposits was 3–4.5, lower than all other 2008 eruptive deposits (Wang et al., 2010). A plausible explanation for these deposits is that they represent erupted lacustrine sediment from the floor of the crater lake. The muddy fall deposits are overlain by massive pyroclastic-flow deposits at least 10 m thick, that contain juvenile pyroclasts of light grey andesite and lithic debris (**Figure 7**). Various types of unburned organic matter (twigs, stems, moss, and grass) are dispersed throughout the lower 1–2 m of the pyroclastic-flow unit in several locations (**Figure 7**). This material represents the vegetated surface on the flanks of the volcano that was overrun and eroded by pyroclastic flows. Wave erosion of the Kasatochi coastline exhumed areas where wooden observation structures had been constructed by biologists working on the island; lumber remains in these areas is also unburned or charred. The presence of unburned organic matter and wood in the basal part of the pyroclastic-flow sequence indicates that these deposits were at low temperature (<300 °C) when emplaced. It is reasonable to conclude that water, water vapor, or both were components of the initial erupting mass and present in significant quantities to cool the eruptive mixture including pyroclastic flows emplaced during the early part of the eruption. As the eruption began to subside and water began reentering the crater, ejection of ballistic particles was noted (Waythomas et al., 2010a). This may have been a result of a greater degree of magma-water interaction as the supply of water increased.

Eruptive removal of the crater lake within the south crater of Korovin volcano was suspected in 2002 and 2004 (McGimsey et al., 2008). The south crater typically hosts a small crater lake

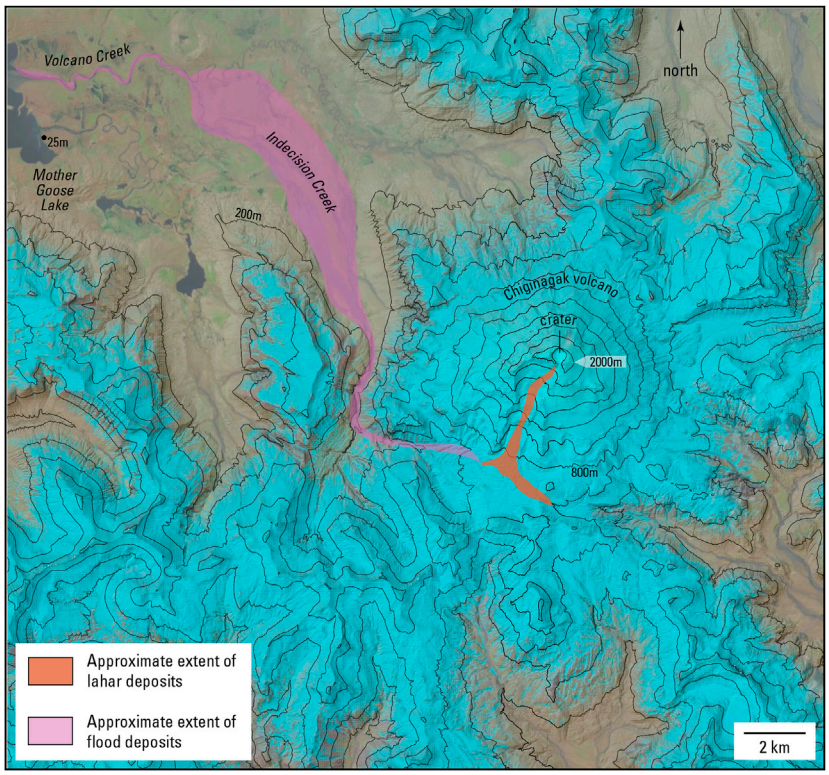

FIGURE 9 | Extent of lahar and flood deposits associated with May 2005 crater lake drainage event at Chiginagak volcano. Modified from Schaefer et al., 2008. Base is Sentinel-2 SWIR image of Chiginagak volcano, May 18, 2021.

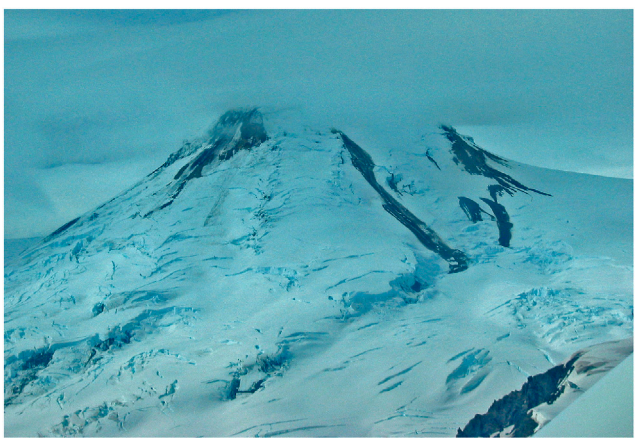

FIGURE 10 | Photograph of the Mount Spurr summit cone, July 15, 2004, view is toward the north. The dark streaks on the upper right (east) side of the cone are small debris flows that emerged through the ice and snow mantling the cone. The largest flow as about 1 km in length. It is unclear if there was a hydrologic connection between these flows and the crater lake that developed within the summit crater (see **Supplementary Figure S1**). Photo by C.A. Neal, AVO.

with an area of about 1.6×10^4 m^2 (**Table 1**; **Supplementary Figure S13**). Images of south crater in 2002 and 2004 show grey, apparently fine-grained deposits on the upper east flank of the cone and these deposits exhibit flowage features (digitate lobes, levees, and shallow channels; **Figure 8**) indicative of water-saturated flow. Brief eruptive bursts at Korovin's south crater are somewhat common historically and are likely phreatic or phreatomagmatic in origin (McGimsey et al., 2008). During these bursts, it is inferred that wet mixtures of ash and debris are emplaced on the upper part of the cone just beyond the crater rim. Although yet unconfirmed with before and after observations, the crater lake is also likely partially or entirely removed during these types of events.

7.2 Lahars

Discharge of water from crater lakes that led to the development of lahars has only been documented a few times in Alaska. The most noteworthy example is at Chiginagak volcano where acidic water drained via an ice dam and produced a lahar and water flood downstream from the crater (**Figure 9**; Schaefer et al., 2008; Schaefer et al., 2013). The volume of water released was about 3.8×10^6 m^3 (Schaefer et al., 2008). Because the fluid component of the flow was acidic (pH at least as low as 2.9) and it liberated acidic aerosols along its flow path, considerable impacts to the riparian ecosystem and to Mother Goose Lake occurred (Schaefer et al., 2008; Schaefer et al., 2013). Apparently, release of acidic water from Chiginagak crater is a recurring event as lake sediment cores from Mother Goose Lake reveal multiple layers

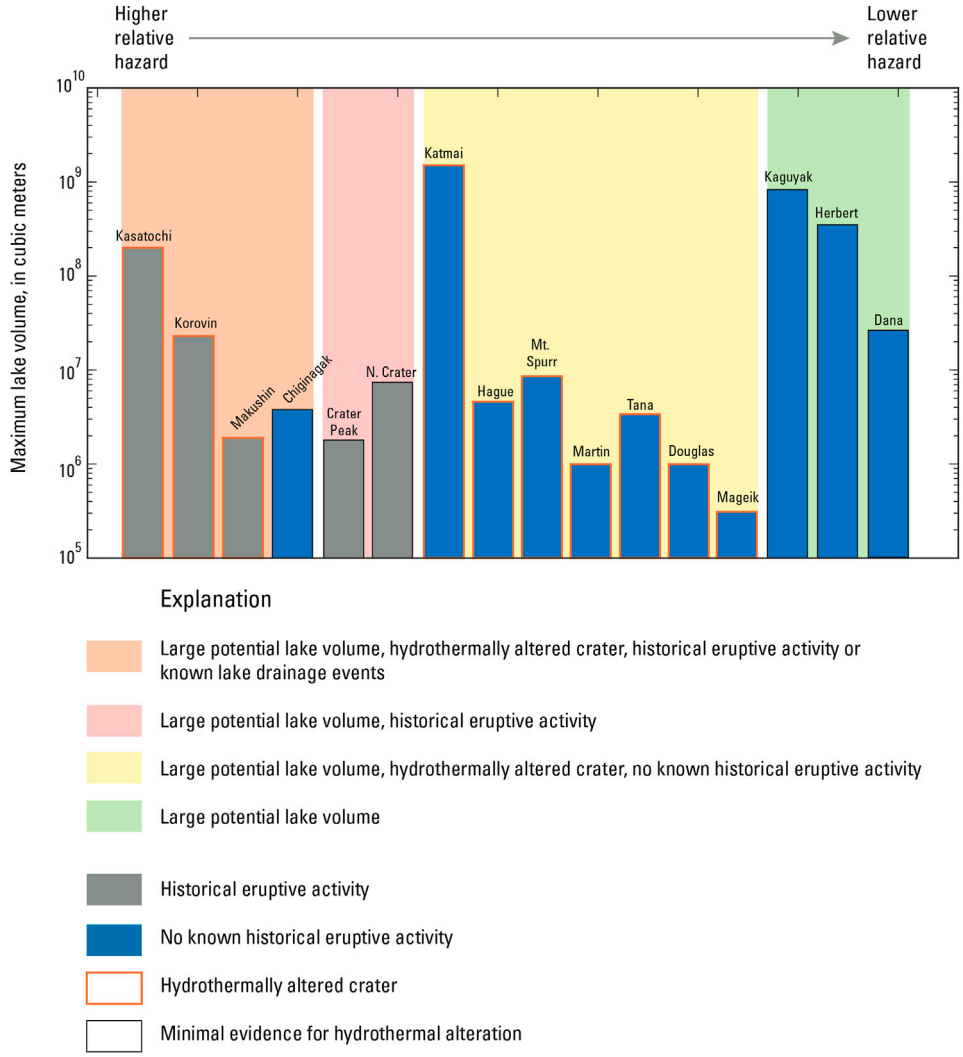

FIGURE 11 | Relative ranking scheme for hydrologic hazards at lake-filled volcanic craters and small calderas in Alaska. Those locations that have hydrothermally altered craters and a record of historical eruptive activity or lake drainage events are more likely to pose greater hydrologic hazards in the future than those locations with minimal evidence for hydrothermal alteration and no known historical eruptive activity.

of orange-colored sediment interpreted as acidic flood deposits (Kassel, 2009).

Watery debris flows were observed on the upper part of the Mount Spurr cone in July 2004 (**Figure 10**). The flows coincided with a period of elevated heat flow at the summit of Mount Spurr that melted a substantial amount of ice and snow at the summit to reveal a summit crater (Coombs et al., 2006). As described in an earlier section of this paper, a small lake developed in the crater. A hydrologic connection between the crater lake and the debris flows observed in July 2004 has not been determined. A plausible explanation for the flows is that they formed by outflow of ponded subglacial water stored on the Mount Spurr edifice that was produced by the elevated heat flow and if so, do not record drainage from the crater lake. Coombs et al. (2006) proposed forceable ejection of water from the crater lake resulting from rapid ice collapse into the water body. For this to occur, a subglacial channel network able to convey the debris-laden water would have to develop either prior to or coincident with ice collapse. Such networks are inferred at the base of thick glaciers (>100 m) but in these situations water release is related to the glacier reaching a flotation condition because of subglacial ponding of water to roughly 0.9 times the ice thickness (Björnsson, 1974; Nye, 1976). The prolonged period of elevated heat flow at the summit of Mount Spurr could have changed the permeability conditions of the snow and ice cover on the edifice such that forceable ejection of water produced the debris flows; however, the hydrologic connection between the crater lake and the flows remains unclear.

7.3 Base Surges

Explosive eruptions through water commonly produce ring-shaped, radially spreading, turbulent clouds known as base surges (Moore, 1967; Waters and Fisher, 1971; Rouwet and Morrissey, 2015). Base

surges move along the surface at speeds on the order of tens of meters per second and can flow as much as 10 km from the eruption site (Mastin and Witter, 2000). Although base surges were observed during the 2016–2017 eruption of Bogoslof volcano (Waythomas et al., 2020) and during the 1977 eruption at Ukinrek Maars (Self et al., 1980), they have not been documented during historical eruptive activity at any of the crater lakes discussed here. It is possible that base surges developed during the 2008 Kasatochi eruption as surge deposits are a component of the sequence of eruptive deposits (Waythomas et al., 2010a; Scott et al., 2010).

8 DISCUSSION AND CONCLUSIONS

Summit craters that contain lakes at stratovolcanoes in Alaska are somewhat uncommon relative to the number of active volcanoes. Of the volcanoes active during the Holocene, only about one-third have summit crater lakes and two of these are small caldera lakes (Katmai, Kaguyak). However, significant amounts of water situated over potentially active vents at the top of volcanic summits with substantial relief augments some of the hazards that are possible at these locations. Although the analysis of floods resulting from failure of the crater rim presented here is based on a worse-case scenario (crater lake at maximum possible volume), excessive volumes of water are not necessary for external water to have a role in affecting eruptive style (Cas and Simmons, 2018). Hydrovolcanic explosions are notoriously violent and when magma-water ratios approach about 5:1 the explosive energy of the mixture reaches a maximum (Wohletz, 1986; Mastin, 1995). Thus, even though a crater lake is shallow, it could supply enough external water to the upper edifice such that water-saturated conditions exist which could promote magma-water interaction possibly increasing the likelihood of explosive phreatomagmatic activity.

Available water in crater lakes in combination with active hydrothermal systems is also a well-known mechanism for enhancing alteration of volcanic edifices (Reid et al., 2001; Heap et al., 2021) which may lead to slope failures and catastrophic crater lake drainage. Several volcanic craters examined here exhibit some degree of hydrothermal alteration, but the extent and type of alteration and strength of the crater walls is not known.

The estimates of maximum peak discharge associated with rapid breach formation through the crater rims indicates that significant water floods could be generated. The flood magnitudes are comparable to the flood peaks associated with large volcanigenic floods in other settings, indicating that Alaskan crater lakes could pose significant hydrologic hazards should the craters become water filled.

The Alaska crater lakes discussed here can be grouped according to the relative hazard posed by each lake (**Figure 11**). The estimated maximum lake volumes for all craters and small calderas indicate that large floods could occur as all locations have large potential lake volumes (**Table 1**). Kasatochi, Korovin, Chiginagak, and Makushin also have hydrothermally altered craters and a record of historical eruptive activity or lake drainage events suggesting that they have a higher relative likelihood of experiencing hydrologic hazards related to their crater lakes. Crater Peak, and north crater on Cerberus volcano have been historically active, which suggests that if lakes develop at these locations, future eruptive activity can have a hydrologic component. Craters and associated lakes at Katmai, Hague, Mount Spurr, Martin, Tana, Douglas, and Mageik have hydrothermally altered craters but no known or limited historical eruptive activity. At these locations non-eruptive mechanisms for crater rim collapse, such as seismically induced liquefaction or seiching, could be important. That these locations have experienced several large historical earthquakes, including the M 9.2 1964 Alaska earthquake without associated crater wall collapse, suggests that the crater walls possess some inherent stability and thus a lower relative hazard potential. Qualitatively, the craters at Kaguyak, Herbert, and Dana appear to be the most stable and thus have the lowest relative crater wall failure hazard.

In comparison to crater lakes elsewhere, there are only a few documented cases of large floods associated with partial degradation of crater rim dams (Yang et al., 2005; Manville, 2015) with Crater Lake at Mt. Ruapehu, New Zealand being the most noteworthy (Massey et al., 2010). Water floods from lakes impounded by calderas have received more study but these are considerably larger than those associated with crater lakes (Waythomas et al., 1996; Manville, 2010). Given the relatively large number of crater lakes in Alaska, additional analysis of crater wall stability, crater hydrology and water balance, and an appropriate monitoring scheme for detecting lake level changes would provide much useful information for improving our understanding of the potential hazards associated with lake-filled volcanic craters.

DATA AVAILABILITY STATEMENT

The original contributions presented in the study are included in the article/**Supplementary Material**, further inquiries can be directed to the corresponding author.

AUTHOR CONTRIBUTIONS

The author confirms being the sole contributor of this work and has approved it for publication.

ACKNOWLEDGMENTS

The author wishes to thank the journal editor, D. Rouwet, two reviewers, C. A. Neal and J. Schaefer for their thoughtful reviews and comments which helped clarify several important points and better focus the manuscript.

SUPPLEMENTARY MATERIAL

The Supplementary Material for this article can be found online at: https://www.frontiersin.org/articles/10.3389/feart.2021.751216/full#supplementary-material

REFERENCES

Belousov, A., and Belousova, M. (2009). Eruptive Process, Effects and Deposits of the 1996 and the Ancient Basaltic Phreatomagmatic Eruptions in Karymskoye Lake, Kamchatka, Russia. *Volcaniclastic Sedimentation in Lacustrine Settings*, 35–60. doi:10.1002/9781444304251.ch3

Björnsson, H. (1974). Explanations of jökulhlaups from Grímsvötn, Vatnajökull, Iceland. *Jökull* 24, 1–26.

Brown, R. D., Brasnett, B., and Robinson, D. (2003). Gridded North American monthly snow depth and snow water equivalent for GCM evaluation. *Atmosphere-Ocean* 41 (1), 1–14. doi:10.3137/ao.410101

Cameron, C. E., and Snedigar, S. F. (2016). Alaska Volcano Observatory image database: *Alaska Div. Geol. Geophys. Surv. Digital Data Ser.* 13. doi:10.14509/29689. https://www.avo.alaska.edu/images/.

Carswell, W. J., Jr. (2013). The 3D Elevation Program: Summary for Alaska. US Geological Survey Fact Sheet FS 2013-3083.

Cas, R. A. F., and Giordano, G. (2014). Submarine volcanism: A review of the constraints, processes and products, and relevance to the Cabo de Gata volcanic succession. *Ijg* 133 (3), 362–377. doi:10.3301/IJG.2014.46

Cas, R. A. F., and Simmons, J. M. (2018). Why deep-water eruptions are so different from subaerial eruptions. *Front. Earth Sci.* 6, 1–21. doi:10.3389/feart.2018.00198

Christenson, B., Németh, K., Rouwet, D., Tassi, F., Vandemeulebrouck, J., and Varekamp, J. C. (2015). "Volcanic Lakes," in *Advances In Volcanology*. Editors D. Rouwet, B. Christenson, F. Tassi, and J. Vandemeulebrouck (Barcelona, Spain: IAVCEI), 1–20. doi:10.1007/978-3-642-36833-2_1

Chwang, A. T., and Housner, G. W. (1978). Hydrodynamic pressures on sloping dams during earthquakes. Part 1. Momentum method. *J. Fluid Mech.* 87 (2), 335–341. doi:10.1017/s0022112078001639

Chwang, A. T. (1978). Hydrodynamic pressures on sloping dams during earthquakes. Part 2. Exact theory. *J. Fluid Mech.* 87 (2), 343–348. doi:10.1017/s0022112078001640

Clague, J. J., and O'Connor, J. E. (2021). "Glacier-related outburst floods," in *Snow and ice-related hazards, risks, and disasters*. Editors W. Haeberli and C. Whiteman (Amsterdam, Netherlands: Elsevier), 467–499. doi:10.1016/b978-0-12-817129-5.00019-6

Clarke, G. K. C. (1982). Glacier Outburst Floods from "Hazard Lake", Yukon Territory, and the Problem of Flood Magnitude Prediction. *J. Glaciol.* 28, 3–21. doi:10.1017/s0022143000011746

Coombs, M. L., Larsen, J. F., and Neal, C. A. (2018). Postglacial Eruptive History and Geochemistry of Semisopochnoi Volcano, Western Aleutian Islands. *US Geol. Surv. Sci. Inv. Rep.*, 2017–5150.

Coombs, M. L., Neal, C. A., Wessels, R. L., and McGimsey, R. G. (2006). Geothermal disruption of summit glaciers at Mount Spurr volcano, 2004-6: An unusual manifestation of volcanic unrest. *US Geol. Surv. Prof. Paper* 1732, 1–33.

Costa, J. E. (1985). Floods from dam failures. *US Geol. Surv. Open-file Rep.* 85–560, 54p. doi:10.3133/ofr85560

Costa, J. E., and Schuster, R. L. (1988). The formation and failure of natural dams. *Geol. Soc. Amer. Bull.* 100 (7), 1054–1068. doi:10.1130/0016-7606(1988)100<1054:tfafon>2.3.co;2

Evans, B. W. C., Bergfeld, D., Neal, C. A., McGimsey, R. G., Werner, C. A., Waythomas, C. F., et al. (2015). Aleutian Arc Geothermal Fluids: Chemical Analyses of Waters and Gases Sampled in Association with the Alaska Volcano Observatory. US Geol. Survey Data Release. doi:10.5066/F78G8HR1

Fenner, C. N. (1930). Mount Katmai and Mount Mageik. *Zeit. F Vulkanol* 13 (1), 1–24.

Fierstein, J., and Hildreth, W. (2008). Kaguyak dome field and its Holocene caldera, Alaska Peninsula. *J. Volcanology Geothermal Res.* 177 (2), 340–366. doi:10.1016/j.jvolgeores.2008.05.016

Finn, C. A., Deszcz-Pan, M., Ball, J. L., Bloss, B. J., and Minsley, B. J. (2018). Three-dimensional geophysical mapping of shallow water saturated altered rocks at Mount Baker, Washington: Implications for slope stability. *J. Volcanology Geothermal Res.* 357, 261–275. doi:10.1016/j.jvolgeores.2018.04.013

Foster, M., Fell, R., and Spannagle, M. (2000). The statistics of embankment dam failures and accidents. *Can. Geotech. J.* 37 (5), 1000–1024. doi:10.1139/t00-030

Francis, P. (1976). *Volcanoes*. Middlesex, England: Penguin, 368 p.

Fread, D. L. (1996). "Dam-Breach Floods," in *Hydrology of Disasters*. Editor V. P. Singh (Dordrecht, Netherlands: Springer), 85–126. doi:10.1007/978-94-015-8680-1_5

Froehlich, D. C. (2008). Embankment dam breach parameters and their uncertainties. *J. Hydraul. Eng.* 134 (12), 1708–1721. doi:10.1061/(asce)0733-9429(2008)134:12(1708)

Gazetas, G. (1987). Seismic response of earth dams: some recent developments. *Soil Dynam. Earthquake Eng.* 6 (1), 3–47. doi:10.1016/0267-7261(87)90008-x

GLIMS Consortium (2005). *GLIMS Glacier Database, Version 1*. Boulder, Colorado USA: NASA National Snow and Ice Data Center Distributed Active Archive Center. doi:10.7265/N5V98602

Heap, M. J., Baumann, T., Gilg, H. A., Kolzenburg, S., Ryan, A. G., Villeneuve, M., et al. (2021). Hydrothermal alteration can result in pore pressurization and volcano instability. *Geology* 49. doi:10.1130/G49063.1

Henderson, F. M. (1966). *Open Channel Flow*. New York: Macmillan, 522 p.

Hildreth, W., and Fierstein, J. (2012b). Eruptive history of Mount Katmai, Alaska. *Geosphere* 8 (6), 1527–1567. doi:10.1130/GES00817.1

Hildreth, W., and Fierstein, J. (2003). Geologic Map of the Katmai Volcanic Cluster, Katmai National Park, Alaska. *US Geol. Surv. Geol. Inv.*, 2778, *Map* I-.

Hildreth, W., Fierstein, J., Lamphere, M. A., and Siems, D. F. (2000). Mount Mageik: A compound stratovolcano in Katmai National Park. *US Geol. Surv. Prof. Paper*, 1912–1615, 23–41.

Hildreth, W., and Fierstein, J. (2012a). The Novarupta-Katmai eruption of 1912 - largest eruption of the twentieth century; centennial perspectives. *US Geol. Surv. Prof.*, 1–278. Paper 1791. doi:10.3133/pp1791

Juhle, W., and Coulter, H. (1955). The Mt. Spurr eruption, July 9, 1953. *Trans. AGU* 36 (2), 199–202. doi:10.1029/tr036i002p00199

Kassel, C. M. (2009). *Lacustrine evidence from Mother Goose Lake of Holocene geothermal activity at Mount Chiginagak, Alaska Peninsula: Flagstaff, Arizona*. Arizona: Northern Arizona University, 138. unpublished M.S. thesis.

Keith, T. E. C. (Editor) (1995). "The 1992 Eruptions of Crater Peak Vent, Mount Spurr Volcano, Alaska." *US Geol. Surv. Bull.*, 2139, 220.

Keith, T. E. C., Thompson, J. M., and McGimsey, R. G. (1995). Chemistry of Crater Lake waters prior to the 1992 eruptions of Crater Peak, Mount Spurr volcano, Alaska. US Geol. Surv. Bull., 2139, 59–63.

Kilgour, G., Manville, V., Della Pasqua, F., Graettinger, A., Hodgson, K. A., and Jolly, G. E. (2010). The 25 September 2007 eruption of Mount Ruapehu, New Zealand: directed ballistics, surtseyan jets, and ice-slurry lahars. *J. Volcanol. Geotherm. Res.* 191 (1-2), 1–14. doi:10.1016/j.jvolgeores.2009.10.015

Kokelaar, B. P. (1983). The mechanism of Surtseyan volcanism. *J. Geol. Soc.* 140 (6), 939–944. doi:10.1144/gsjgs.140.6.0939

Kokelaar, P. (1986). Magma-water interactions in subaqueous and emergent basaltic. *Bull. Volcanol.* 48 (5), 275–289. doi:10.1007/BF01081756

Larsen, J. F., Neal, C. A., Schaefer, J. R., Kaufman, A. M., and Lu, Z. (2015). The 2008 phreatomagmatic eruption of Okmok volcano, Aleutian Islands, Alaska: Chronology, deposits, and landform changes. State of Alaska, Division of Geological and Geophysical Surveys Report of Investigations 2015-2, 52.

Lecointre, J., Hodgson, K., Neall, V., and Cronin, S. (2004). Lahar-triggering mechanisms and hazard at Ruapehu volcano, New Zealand. *Nat. Hazards* 31 (1), 85–109. doi:10.1023/B:NHAZ.0000020256.16645.eb

Lyu, Z., Chai, J., Xu, Z., Qin, Y., and Cao, J. (2019). A Comprehensive Review on Reasons for Tailings Dam Failures Based on Case History. *Adv. Civil Eng.* 2019, 1–18. doi:10.1155/2019/4159306

MacDonald, T. C., and Langridge-Monopolis, J. (1984). Breaching Charateristics of Dam Failures. *J. Hydraulic Eng.* 110 (5), 567–586. doi:10.1061/(asce)0733-9429(1984)110:5(567)

Manville, V. (2010). An overview of break-out floods from intracaldera lakes. *Glob. Planet. Change* 70 (1–4), 14–23. doi:10.1016/j.gloplacha.2009.11.004

Manville, V., Hodgson, K. A., and Nairn, I. A. (2007). A review of break-out floods from volcanogenic lakes in New Zealand. *New Zealand J. Geology Geophys.* 50 (2), 131–150. doi:10.1080/00288300709509826

Manville, V. (2015). "Volcano-Hydrologic Hazards from Volcanic Lakes," in *Volcanic Lakes*. Editors D. Rouwet, B. Christenson B., F. Tassi, and J. Vandemeulebrouck (Berlin, Heidelberg: Springer), 21–71. Advances in Volcanology. doi:10.1007/978-3-642-36833-2_2

March, R., Mayo, L. R., and Trabant, D. (1997). Snow and ice volume on Mount Spurr Volcano, Alaska, 1981. *US Geol. Surv. Water-res. Inv. Rep. WRI* 97-4142, 362. plates, scale 1:50,000. doi:10.3133/wri974142

Massey, C. I., Manville, V., Hancox, G. H., Keys, H. J., Lawrence, C., and McSaveney, M. (2010). Out-burst flood (lahar) triggered by retrogressive landsliding, 18 March 2007 at Mt Ruapehu, New Zealand-a successful early warning. *Landslides* 7 (3), 303–315. doi:10.1007/s10346-009-0180-5

Mastin, L. G. (1995). Thermodynamics of gas and steam-blast eruptions. *Bull. Volcanol.* 57 (2), 85–98. doi:10.1007/bf00301399

Mastin, L. G., and Witter, J. B. (2000). The hazards of eruptions through lakes and seawater. *J. Volcanology Geothermal Res.* 97, 195–214. doi:10.1016/s0377-0273(99)00174-2

McGarr, A., and Vorhis, R. C. (1968). Seismic seiches from the March 1964 Alaska earthquake. *US Geol. Surv. Prof.* Paper 544–E, 43 p., 1 sheet, scale 1:5,000,000. doi:10.3133/pp544e

McGimsey, R. G., and Neal, C. A. (1996). 1995 volcanic activity in Alaska and Kamchatka: summary of events and response of the Alaska Volcano Observatory: U.S. *Geol. Surv. Open-File Rep.* 96-0738, 22.

McGimsey, R. G., Neal, C. A., Dixon, J. P., and Ushakov, S. (2008). Volcanic activity in Alaska, Kamchatka, and the Kurile Islands: Summary of events and response of the Alaska Volcano Observatory. *US Geol. Surv. Sci. Inv. Rep.* 2007-5269, 94.

McGimsey, R. G., Neal, C. A., and Girina, O. (2003). 1998 volcanic activity in Alaska and Kamchatka: Summary of events and response of the Alaska Volcano Observatory. *US Geol. Surv. Open-file Rep. 03* 423, 35.

McGimsey, R. G., Maharrey, J. Z., and Neal, C. A. (2014). 2011 volcanic activity in Alaska: Summary of events and response of the Alaska Volcano Observatory. US Geol. Surv. Sci. Inv. Report 2014-5159, 49.

Miller, T. P., McGimsey, R. G., Richter, D. H., Riehle, J. R., Nye, C. J., Yount, M. E., et al. (1998). Catalog of the historically active volcanoes of Alaska. *US Geol. Surv. Open-file Rep.* 98-0582, 104. doi:10.3133/ofr98582

Moore, J. G. (1967). Base surge in recent volcanic eruptions. *Bull. Volcanol.* 30 (1), 337–363. doi:10.1007/bf02597678

Moore, J. G., Nakamura, K., and Alcaraz, A. (1966). The 1965 eruption of Taal Volcano. *Science* 151, 955–960. doi:10.1126/science.151.3713.955

Morrissey, M., Gisler, G., Weaver, R., and Gittings, M. (2010). Numerical model of crater lake eruptions. *Bull. Volcanol.* 72 (10), 1169–1178. doi:10.1007/s00445-010-0392-5

Motyka, R. I., Queen, L. D., Janik, C. J., Sheppard, D. S., Poreda, R. J., and Liss, S. A. (1988). Fluid geochemistry and fluid mineral equilibria in test wells and thermal gradient holes at the Makushin geothermal area, Unalaska Island, Alaska. *Alsk. Div. Geol. Geophys. Surv. Rep. Inv.* 88-14, 90.

Motyka, R. I. (1978). *Surveillance of Katmai caldera and crater lake, Alaska*. US: Unpub. Report to U.S. Park Service, University of Alaska Fairbanks Geophysical Institute Report UAG-R, 19. PX9100-7-1009.

Motyka, R. J., Liss, S. A., Nye, C. J., and Moorman, M. A. (1993). Geothermal resources of the Aleutian Arc. *Alsk. Div. Geol. Geophys. Surv. Prof. Rep. PR* 0114, 17, p., 4 sheets, scale 1:1,000,000.

Neal, C. A., McGimsey, R. G., Miller, T. P., Riehle, J. R., and Waythomas, C. F. (2001). Preliminary volcano-hazard assessment for Aniakchak Volcano, Alaska. US Geol. Surv. Open-File Report 00-0519, 35.

Neall, V. E. (1996). "Hydrological disasters associated with volcanoes," in *Hydrology of disasters*. Editor V. P. Singh (Dordrecht: Springer), 395–425.

Németh, K., Cronin, S. J., Charley, D., Harrison, M., and Garae, E. (2006). Exploding lakes in Vanuatu - "Surtseyan-style" eruptions witnessed on Ambae Island. *Episodes* 29 (2), 87–92. doi:10.18814/epiiugs/2006/v29i2/002

Newhall, C. G., and Dzurisin, D. (1988). Historical unrest at large calderas of the world. *US Geol. Surv. Bull.* 1855, 1108. doi:10.3133/b1855

Nye, C. J., Scott, W. E., Neill, O. K., Waythomas, C. F., Cameron, C. E., and Calvert, A. T. (2017). Geology of Kasatochi volcano, Aleutian Islands, Alaska. *Alsk. Div. Geol. Geophys. Surv. Prof. Rep.* 123, 127, p., 1 sheet, scale 1:5000. doi:10.14509/29718

Nye, C. J., and Turner, D. L. (1990). Petrology, geochemistry, and age of the Spurr volcanic complex, eastern Aleutian Arc. *Bull. Volcanol.* 52 (3), 205–226. doi:10.1007/bf00334805

Nye, J. F. (1976). Water Flow in Glaciers: Jökulhlaups, Tunnels and Veins. *J. Glaciol.* 17 (76), 181–207. doi:10.1017/s002214300001354x

O'Connor, J. E., and Costa, J. E. (2004). The world's largest floods, past and present: their causes and magnitudes. *US Geol. Surv. Circ.* 1254, 13p. doi:10.3133/cir1254

Pasternack, G. B., and Varekamp, J. C. (1997). Volcanic lake systematics I. Physical constraints. *Bull. Volcanology* 58 (7), 528–538. doi:10.1007/s004450050160

Pelecanos, L., Kontoe, S., and Zdravković, L. (2013). Numerical modelling of hydrodynamic pressures on dams. *Comput. Geotechnics* 53, 68–82. doi:10.1016/j.compgeo.2013.04.003

Persico, L., Lanman, H., Loopesko, L., Bruner, K., and Nicolaysen, K. (2019). Geomorphic processes influence human settlement on two islands in the Islands of Four Mountains, Alaska. *Quat. Res.* 91 (3), 953–971. doi:10.1017/qua.2018.112

Reid, M. E., Sisson, T. W., and Brien, D. L. (2001). Volcano collapse promoted by hydrothermal alteration and edifice shape, Mount Rainier, Washington. *Geol.* 29 (9), 779–782. doi:10.1130/0091-7613(2001)029<0779:vcpbha>2.0.co;2

Riehle, J. R. (1985). A reconnaissance of the major Holocene tephra deposits in the upper Cook Inlet region, Alaska. *J. Volcanol. Geotherm. Res.* 26 (1-2), 37–74. doi:10.1016/0377-0273(85)90046-0

Rouwet, D., and Morrissey, M. M. (2015). "Mechanisms of Crater Lake Breaching Eruptions," in *Volcanic Lakes*. Editors D. Rouwet, B. Christenson B., F. Tassi, and J. Vandemeulebrouck (Berlin, Heidelberg: Springer), 73–91. Advances in Volcanology. doi:10.1007/978-3-642-36833-2_210.1007/978-3-642-36833-2_3

Rouwet, D., Taran, Y. A., and Varley, N. R. (2004). Dynamics and mass balance of El Chichón crater lake, Mexico. *Geofisica Internacional* 43 (3), 427–434.

Rouwet, D. (2021). "Volcanic lake dynamics and related hazards," in *Hazards and Disasters, Forecasting and Planning for Volcanic Hazards, Risks, and Disasters*. Editor P. Papale (Amsterdam: Elsevier), v. 2, 439–471. doi:10.1016/b978-0-12-818082-2.00011-1

Schaefer, J. R., Scott, W. E., Evans, W. C., Wang, B., and McGimsey, R. G. (2013). Summit crater lake observations, and the location, chemistry, and pH of water samples near Mount Chiginagak volcano, Alaska: 2004-2012. *Alsk. Div. Geol. Geophys. Surv. Rep. Inv.* 6 (2), 25. doi:10.14509/25602

Schaefer, J. R., Scott, W. E., and Layer, P. W. (2017). Geologic map of Mount Chiginagak volcano, Alaska. *Alsk. Div. Geol. Geophys. Surv. Rep. Inv* 10, 32, p., 1 sheet, scale 1:25,000. doi:10.14509/29769

Schaefer, J. R., Scott, W. E., Evans, W. C., Jorgenson, J., McGimsey, R. G., and Wang, B. (2008). The 2005 catastrophic acid crater lake drainage, lahar, and acidic aerosol formation at Mount Chiginagak volcano, Alaska, USA: Field observations and preliminary water and vegetation chemistry results. *Geochem. Geophys. Geosyst.*, 9(7), a, n p., doi:10.1029/2007GC001900

Scott, W. E., Nye, C. J., Waythomas, C. F., and Neal, C. A. (2010). August 2008 Eruption of Kasatochi Volcano, Aleutian Islands, Alaska-Resetting an Island Landscape. *Arctic, Antarctic, Alpine Res.* 42 (3), 250–259. doi:10.1657/1938-4246-42.3.250

Self, S., Kienle, J., and Huot, J. P. (1980). Ukinrek Maars, Alaska: II, Deposits and formation of the 1977 craters. *J. Volcanol. Geotherm. Res.* 7 (1-2), 39–65. doi:10.1016/0377-0273(80)90019-0

Singh, V. P., Scarlatos, P. D., Collins, J. G., and Jourdan, M. R. (1988). Breach erosion of earthfill dams (BEED) model. *Nat. Hazards* 1 (2), 161–180. doi:10.1007/bf00126613

Stafford, J. M., Wendler, G., and Curtis, J. (2000). Temperature and precipitation of Alaska: 50 year trend analysis. *Theor. Appl. Climatology* 67 (1–2), 33–44. doi:10.1007/s007040070014

Stelling, P., Gardner, J. E., and Begét, J. (2005). Eruptive history of Fisher Caldera, Alaska, USA. *J. Volcanology Geothermal Res.* 139 (3–4), 163–183. doi:10.1016/j.jvolgeores.2004.08.006

Strehlow, K., Sandri, L., Gottsmann, J. H., Kilgour, G., Rust, A. C., and Tonini, R. (2017). Phreatic eruptions at crater lakes: occurrence statistics and probabilistic hazard forecast. *J. Appl. Volcanol.* 6, 4. doi:10.1186/s13617-016-0053-2

Sturm, M., Taras, B., Liston, G. E., Derksen, C., Jonas, T., and Lea, J. (2010). Estimating snow water equivalent using snow depth data and climate classes. *J. Hydromet.* 11 (6), 1380–1394. doi:10.1175/2010JHM1202.1

Sykes, L. R., Kisslinger, J. B., House, L., Davies, J. N., and Jacob, K. H. (1981). Rupture zones and repeat times of great earthquakes along the Alaska-Aleutian Arc, 1784–1980. *Earthquake Prediction: Int. Rev.* 4, 73–80.

Walder, J. S., and O'Connor, J. E. (1997). Methods for predicting peak discharge of floods caused by failure of natural and constructed earthen dams. *Water Resour. Res.* 33 (10), 2337–2348. doi:10.1029/97wr01616

Wang, B., Michaelson, G., Ping, C.-L., Plumlee, G., and Hageman, P. (2010). Characterization of Pyroclastic Deposits and Pre-eruptive Soils following the 2008 Eruption of Kasatochi Island Volcano, Alaska. *Arctic, Antarctic, Alpine Res.* 42, 276–284. doi:10.1657/1938-4246-42.3.276

Waters, A. C., and Fisher, R. V. (1971). Base surges and their deposits: Capelinhos and Taal Volcanoes. *J. Geophys. Res.* 76 (23), 5596–5614. doi:10.1029/JB076i023p05596

Watters, R. J., Zimbelman, D. R., Bowman, S. D., and Crowley, J. K. (2000). Rock mass strength assessment and significance to edifice stability, Mount Rainier and Mount Hood, Cascade Range volcanoes. *Pure Appl. Geophys.* 157 (6), 957–976. doi:10.1007/s000240050012

Waythomas, C. F., Angeli, K., and Wessels, R. L. (2020). Evolution of the submarine–subaerial edifice of Bogoslof volcano, Alaska, during its 2016–2017 eruption based on analysis of satellite imagery. *Bull. Volc.* 82 (2), 1–26. doi:10.1007/s00445-020-1363-0

Waythomas, C. F. (2015). Geomorphic consequences of volcanic eruptions in Alaska: A review. *Geomorphology* 246, 123–145. doi:10.1016/j.geomorph.2015.06.004

Waythomas, C. F., Pierson, T. C., Major, J. J., and Scott, W. E. (2013). Voluminous ice-rich and water-rich lahars generated during the 2009 eruption of Redoubt Volcano, Alaska. *J. Volcanology Geothermal Res.* 259, 389–413. doi:10.1016/j.jvolgeores.2012.05.012

Waythomas, C. F., Scott, W. E., and Nye, C. J. (2010b). The geomorphology of an Aleutian volcano following a major eruption: the 7-8 August 2008 eruption of Kasatochi Volcano, Alaska, and its aftermath. *Arctic, Antarctic, Alpine Res.* 42 (3), 260–275. doi:10.1657/1938-4246-42.3.260

Waythomas, C. F., Scott, W. E., Prejean, S. G., Schneider, D. J., Izbekov, P., and Nye, C. J. (2010a). The 7–8 August 2008 eruption of Kasatochi Volcano, central Aleutian Islands, Alaska. *J. Geophys. Res. Solid Earth* 115, B12. doi:10.1029/2010jb007437

Waythomas, C. F., Walder, J. S., McGimsey, R. G., and Neal, C. A. (1996). A catastrophic flood caused by drainage of a caldera lake at Aniakchak Volcano, Alaska, and implications for volcanic hazards assessment. *Geol. Soc. Am. Bull.* 108 (7), 861–871. doi:10.1130/0016-7606(1996)108<0861:ACFCBD>2.3.CO;2

Werner, C. A., Kern, C., and Kelly, P. J. (2020). Chemical Evaluation of Water and Gases Collected from Hydrothermal Systems Located in the Central Aleutian Arc. *US Geol. Surv. Sci. Inv. Rep.* 5043, 35.

Wesson, R. L., Boyd, O. S., Mueller, C. S., Bufe, C. G., Frankel, A. D., and Petersen, M. D. (2007). Revision of time-independent probabilistic seismic hazard maps for Alaska. *US Geol. Surv. Open-file Rep*. 1043, 33 p. doi:10.3133/ofr20071043

Wilson, F. H., Detterman, R. L., Miller, J. W., and Case, J. E. (1995). Geologic map of the Port Moller, Stepovak Bay, and Simeonof Island quadrangles, Alaska Peninsula, Alaska. *US Geol. Surv. Misc. Invest. Ser. Map* 2272, 2, sheets, scale 1: 250,000.

Wohletz, K. H. (1986). Explosive magma-water interactions: Thermodynamics, explosion mechanisms, and field studies. *Bull. Volcanol.* 48, 245–264. doi:10.1007/bf01081754

Wohletz, K., Zimanowski, B., Büttner, R., and Fagents, S. A. (2009). "Magma-water interactions," in *Modeling Volcanic Processes: The Physics and Mathematics of Volcanism*. Editors S. A. Fagents, T. K. P. Gregg, and R. M. C. Lopes (Cambridge, United Kingdom: Cambridge Univ. Press), 230–257. doi:10.1017/CBO9781139021562.011

Wolfe, B. A. (2001). *Paleohydrology of a catastrophic flood release from Okmok caldera and post-flood eruption history at Okmok volcano, Umnak Island*. Alaska: University of Alaska-Fairbanks, Ph.D. Dissertation, 100 p.

Yang, P., Yokoyama, N., Inoue, K., and Amino, K. (2005). Preliminary Investigation of the Crater Lake Breach at Mt. Pinatubo, Philippines. *J. Jpn. Soc. Eng. Geology* 46 (5), 287–292. doi:10.5110/jjseg.46.287

Conflict of Interest: The author declares that the research was conducted in the absence of any commercial or financial relationships that could be construed as a potential conflict of interest.